University of Manitoba
Department of Electrical & Computer Engineering

ECE 4600 Group Design Project

Final Project Report

Acquisition System of S-Parameters for the Microwave Imaging of a Grain Bin

by
Group 07

Dimitri Anistratov
Shucheng Gu
Edinam Tettevi
Robert Brandt
Kathy Nguyen

Academic Supervisor
Joe Lovetri

Co-Supervisor
Mohammad Asefi

Industry Supervisors
Ian Jeffrey – Academic Supervisor
Paul Card – 151 Research Inc
Colin Gilmore – 151 Research Inc

Date of Submission
March 4, 2015

Copyright © 2015 Dimitri Anistratov, Robert Brandt, Shucheng Gu, Kathy Nguyen, Edinam Tettevi,

Abstract

This report describes the design and implementation of a s-parameter data acquisition system for the use in a commercial grain storage bin. The system is divided into the following components which will be described in detail in this report: An RF multiplexer, a VNA, a microcomputer and an array of magnetic and electric field antennas. The s-parameter data that is collected by the system will be used by the Electromagnetic Imaging lab at the University of Manitoba to create an image of the dielectric contents of the grain bin. This microwave imaging technique will be used to detect moisture and grain spoilage inside the grain storage unit which in turn offers farmers a way to protect their stock in order to maximize profits.

Contributions

This project aims to create an affordable and user friendly solution for the detection of spoilage and moisture of grain inside of an industrial grain storage bin. This can be achieved through microwave imaging of the contents of the bin and reproducing a three dimensional image of the different dielectric contents of the bin. A typical microwave imaging system consists of a VNA, an RF multiplexer an array of antennas and a data acquisition and processing unit. The design and testing of these individual components was distributed among the group members as described below.

Another major contributor to this project was PhD student Mohammad Asefi, who worked closely with our group and provided helpful academic and technical advice.

	Dimitri Anistratov	Robert Brandt	Shucheng Gu	Kathy Nguyen	Edinam Tettevi
Electric field antenna design, simulation and testing			●		
Magnetic field antenna design simulation and testing	●				
Raspberry pi user interface and automation software				●	
VNA control software				●	
RF component of multiplexer PCB design and layout		●			
DC component of multiplexer PCB design and layout					●
Multiplexer address decoding					●
ESD protection		○			●
VNA and RF multiplexer Performance testing	○			○	

Legend: ● Lead task ○ Contributed

Acknowledgements

We would first like to thank our academic supervisors Dr. Joe LoVetri and Mohammad Asefi for providing us with constant technical and academic help and support throughout the duration of the project, and for providing us with access to necessary equipment, materials and parts required for this project. Thanks to Zoran Trajkoski with helping us with all of our PCB antenna prototyping and support, thank you to Sinisa Janjic with part ordering. We would also like to thank Paul Card and Colin Gilmore, our industry sponsors at 151 Research Inc. with the opportunity to work on this project.

Table of Contents

Abstract i
Contributions ii
Acknowledgments iv
List of Figures viii
List of Tables x
List of Abbreviations xi
Definitions xii

1 Introduction 1
  1.1 Purpose 1
  1.2 Design overview 1
  1.3 Design specifications 2

2 Antennas 3
  2.1 E-field Antenna 3
    2.1.1 Research and Preliminary Design 4
    2.1.2 Antenna Building and Testing 9
  2.2 H-field Antenna 14
    2.2.1 Purpose 14
    2.2.2 Research 15
    2.2.3 Design 15

2.2.4 PCB Antenna Design 17
2.2.5 PCB Antenna Simulation 17
2.2.6 Simulation Results 18
2.2.7 PCB Layout 20
2.2.8 H-field Antenna Testing 21
2.2.9 G-TEM Test Results 22

3 Multiplexer 24
3.1 RF Switch 24
3.1.1 Background 24
3.1.2 Design 25
3.2 DC Switching 31
3.2.1 Hardware 31
3.2.2 ESD Protection 36

4 Vector Network Analyzer 37
4.1 Harware Specifications 37
4.2 Calibration and Testing 39
4.3 miniVNA PRO Software 41

5 Microprocessor 42
5.1 Hardware Integration 42
5.2 Software Design and Integration 43
5.2.1 Initialization Process 44
5.2.2 Data Acquisition Process 44
5.2.3 Post-Data Processing 45
5.2.4 Data Transmission Process 47
5.3 Software Setup and Configuration 47

5.3.1 Prerequisites 48
5.3.2 Configuration Parameters 50

6 Future Work 52
6.1 Software 52
6.2 RF Multiplexer Module 53
6.3 Antennna 53

7 Conclusions 54

References 56

Appendix A Appendix A 58

Appendix B Appendix B 60
B.1 gbin.sh 60
B.2 put2str.cs 62
B.3 button.py 64
B.4 Dropbox Setup on the Raspberry Pi 2 65
B.4.1 Setup Instructions 65
B.4.2 'dropbox-uploader.sh' Commands 65

Appendix C Appendix C 67

Appendix D Appendix D 68

Appendix E Curriculum Vitae 70

List of Figures

2.1 equivalent model of meander line sections 5
2.2 meandered monopole antenna geometry 6
2.3 Resonant frequency of meandered line antenna M0 to M5 6
2.4 resonant frequency vs meandered spacing 7
2.5 Bending angle when α= 45,60,75,90,120 degree conditions 7
2.6 the relation between bending angle and resonant frequency 8
2.7 radiation principle of a 90 degree bending meandered antenna 8
2.8 final antenna view 9
2.9 S11 curve for meandered antenna in HFSS 10
2.10 S11 curve for real testing results 11
2.11 S12 curve for cross-plane polarization in HFSS 11
2.12 S12 curve for co-plane polarization in HFSS 12
2.13 S12 for cross-plane polarization in real test 13
2.14 S12 for co-plane polarization in real test 13
2.15 shielded loop antenna [4] 16
2.16 prototype antenna 17
2.17 HFSS model of PCB antenna 18
2.18 S11 simulated 19
2.19 S11 of actual antenna 19
2.20 E distribution with shielding 20

2.21 E distribution Shielding removed 20
2.22 fabricated antenna 21
2.23 field lines in G-TEM for reference 21
2.24 E-orientation 22
2.25 H-orientation 23
3.1 Multiplexer connecting VNA to antenna array 25
3.2 Initial design of the multiplexer 26
3.3 Final design of the multiplexer 27
3.4 PCB layout for SP3T board 27
3.5 PCB layout for top layer of SP8T and SPDT board 28
3.6 PCB layout for bottom layer of SP8T and SPDT board 29
3.7 Stack up for PCBs in Altium 29
3.8 Topology for the integration between DC and RF Switches 32
3.9 Initial DC Switch Design for Matrix Switch Design 33
3.10 Final DC Switch Design for Multi-Layer RF Switch Design 34
4.1 miniVNA PRO calibration software. 39
4.2 S11 measurement(real) for both VNAS. 40
4.3 miniVNA PRO open port measurement in reflection mode. 40
4.4 miniVNA PRO Software Output 41
5.1 LED and Button Circuit 43
5.2 S-Parameter Data Acquisition system processes. 44
5.3 Flow chart of the Data Acquisition Process. 45
5.4 Flow Chart of Post-Data Processing Procedure. 46
C.1 Raspberry Pi 2 Pinout [12]. 67
D.1 69

List of Tables

2.I specification of the E-filed antenna . . . 3
4.I VNA Requirements [7] . . . 38
4.II miniVNA PRO Specifications . . . 38
5.I Raspberry Pi 2 Specifications [8] . . . 42
5.II Required files in the /root/grainbin directory of the Raspberry Pi 2. . . . 48
5.III Required packages to be installed on Arch Linux OS running on the Raspberry Pi 2. 48
5.IV Parameter definitions for 'gbin.sh'. . . . 50
5.V Parameter definitions for miniVNA PRO software command. . . . 51
A.I Project Budget . . . 59

List of Abbreviations

Abbreviation	Description
RPi2	Raspberry Pi 2
SPDAQ	S-Parameter Data Acquisition
MVP	miniVNA PRO
RF mux	RF multiplexer
MWI	Microwave Imaging

Definitions

VNA	Vector Network Analyzer
RF	Radio Frequency
E	Electric
H	Magnetic
λ	Wavelength
PEC	Perfect electric conductor
PCB	Printed circuit board
EIL	Electromagnetic Imaging Lab
EM	Electromagnetic
ESD	Electrostatic discharge
TEM	Transverse electric magnetic
HFSS	High frequency structure simulator
PC	Personal computer
IC	Integrated circuit

ϵ_r	Relative Permittivity
γ	Propagation constant
ω	Frequency in radians
μ	Permeability
α	Angle
θ	Phase in degrees
DC	Direct current
SPDT	Single pole dual throw
SP3T	Single pole three throw
SP8T	Single pole eight throw
prepreg	Pre-impregnated thermoplastic resin
CLI	Command line interface
SSH	Secure shell protocol
SFTP	Secure file transfer protocol
IP	Internet protocol
SPI	Serial peripheral interface
GPIO	General purpose input output
GUI	Graphical User Interface
UI	User Interface

Chapter 1

Introduction

1.1 Purpose

The Canadian farm industry is a multibillion dollar a year industry which needs to provide for a growing human population. High production of grain requires farmers to dry and store the grains that they grow, however this introduces problems such as possible spoilage of the grain as well as proper humidity control. Spoilage and water has dielectric properties which are different of those that dry good grain has, therefore these anomalies can be detected with the use of a microwave imaging system which consists of a Vector Network Analyzer, a 2xN RF multiplexer, an N array of antennas and a computer for collecting and analyzing the scattered parameters to create a three dimensional image of a material. However typical microwave imaging systems are very costly and complex which does not provide a feasible solution for farmers, costing in the magnitude of hundreds of thousands of dollars.

1.2 Design overview

Our project is aimed at researching into and developing a better topology for the acquisition of s-parameter data from a grain bin. These parameters of the bin's contents can then be analyzed to produce an image that displays the grains dielectric permittivity properties to detect water contamination. To accomplish our goal, the project was broken into a research phase, a design and integration phase and finally, a calibration and field testing phase. These phases would be responsible for a well rectified integration between 16 E-field and H-field antennas, a DC/RF multiplexer switch box, a microcomputer, a microcontroller and a portable vector network analyzer (VNA).

The array of 16 antennas, consisting of both E-field and H-field antennas, will be built and installed in a full size grain bin. A 2-port VNA, via the use of a microcomputer, will transmit a signal though a microcontroller which controls the RF multiplexer switch box to a single antenna and then receive the scattered signal back through each one of the other antennas. The microcomputer will then collect and format the received data such that it can be processed later to create an image of the grain bin's contents on an external PC.

1.3 Design specifications

The system has to be affordable yet accessible so that it can be used by the targeted consumer who are grain farmers. The antennas used in the bin would have to be miniaturized and easily manufacture-able. At least 16 antennas with the possibility of 2 types will need to be produced. The RF switch that links the antennas to the VNA needs to have some sort of discharge protection, a minimum of 24 switching ports with relatively low noise and insertion loss. The processes need to be automated with the push of a button which offers an ease of use for the user.

Chapter 2

Antennas

2.1 E-field Antenna

The data acquisition system of a grain bin is based on the use of microwave imaging system to estimate the dielectric properties of the material in the grain bin. As explained in the section of introduction. The object of the antenna is to receive or transmit scattering parameter data to local PC for analyzing propose.

Table 2.I: specification of the E-filed antenna

Specifications	Value
Resonant frequency	70MHz - 90MHz
S_{11} at operating frequency	Below -6dB
Antenna size	Maximum 10×15 cm
Co-plane and cross-plane polarization difference	At least 15dB
Number of antennas in an array	24

In the previous MWI system, the straight line monopole antenna with a total length of 1m is used inside the bin, however, in the resonant chamber each antenna size cannot exceed a 10*15 cm due to the volume limitation of the inner space. After investigating several options focusing on classes of small patch antennas, a suitable and feasible method has come up as meandered monopole antenna printed on a PCB layer. The FR4 with $\epsilon_r = 4.4$ will be used as the dielectric substrate of the PCB board.

2.1.1 Research and Preliminary Design

We will start the design process from the researching and simulating the features of the simple straight line monopole antenna, then we need to determine the parameters of the meandered antenna in order to increase numbers of meandered sections to satisfy the size requirement.

The following parameters we need to consider:

- Numbers of meander sections
- Spacing of meander sections
- Bending angles for each section

A simple single straight line monopole antenna can be represented using an equivalent inductor circuit model in Figure 2.1. If an additional equivalent component is added up to the self-inductance of the antenna, the resonant frequency of the meander line will be relatively change compared with previous antenna with same height, this method will provide us a reasonable approximation of the working principle of this class of antenna.

Next we need to demonstrate several simulations and optimizations to figure out how the meander line configurations will change the performance of the antenna return loss curve (S11), radiation patterns in terms of the parameters given above. In these cases, it is predicted that the inductor circuit model will not be adequate for explaining the relative changes of the resonant frequencies[1].

Since the self-resonant frequency of the simple straight line monopole antenna can be modeled as the inductor circuit model, we can use the formula (2.1) to calculate the self-inductance when the total physical length of the antenna is about $\lambda/4$.

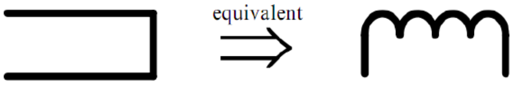

Fig. 2.1: equivalent model of meander line sections

$$Ls = \frac{\mu}{\pi}0.2384\lambda(ln(4\frac{0.2384\lambda}{d} - 1)) \tag{2.1}$$

Where d is the diameter of the radiator of the antenna and λ is the required resonant wavelength, the resonant frequency of the antenna can be estimated using an inductor circuit model representation as introduced in Figure 2.1. To determine the inductance in each meandered section, we will use an equivalent transmission line model which has a characteristic impedance given as

$$Z_0 = 276log(\frac{2s}{d}) \tag{2.2}$$

where s is the spacing between each meandered section, as a result, the equivalent inductance of each section, Lm, is given as following:

$$Lm = \frac{|Z_0tanh(\gamma l)|}{\omega} \tag{2.3}$$

Where is the propagation factor of free space, l is the length of each meandered section and is angular velocity, the resonant frequency of the meandered line antenna should have same physical length as the simple straight line monopole antenna, but we need to replace the equivalent inductor Ls by the sum of Ls+NLm, where N is the number of meander sections.

In order to exam the resonant behavior of the meandered line antenna, we will simulate and use optimism method in HFSS to compare each group of meandered antenna parameters given above. M0 to M5 configurations shown in Figure 2.2 (Best, Morrow) is applied to observe the variation the resonant frequency of the antenna [2][3].

The M0 configuration has a self-resonant frequency at 80MHz, while the M5 configuration

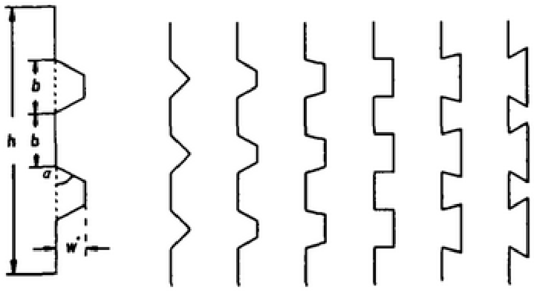

Fig. 2.2: meandered monopole antenna geometry

has a self-resonant frequency at 110MHz. For antenna represented in 2.1, s is equal to 1cm, L is equal to 4cm, using equation (2.2) and (2.3), and the value of Lm is calculated as about 300nH, a comparison table of resonant behavior of different numbers of section is listed in Figure 2.3.

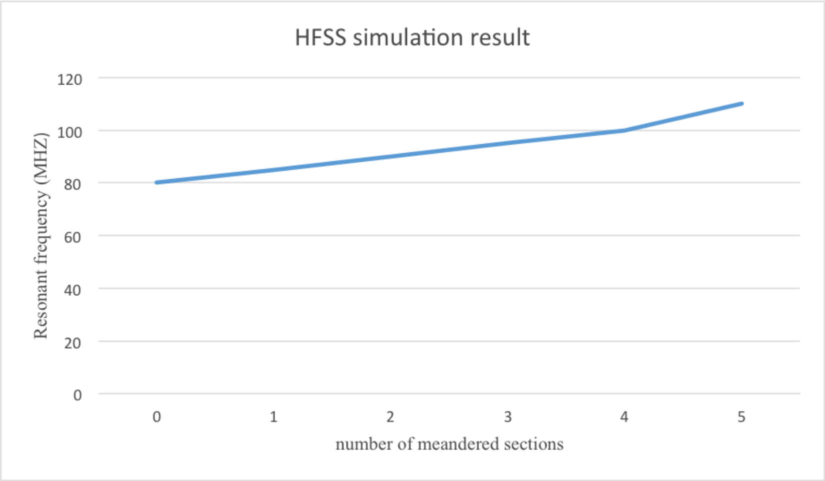

Fig. 2.3: Resonant frequency of meandered line antenna M0 to M5

From Figure 2.3, it is evident that the inductor circuit model representing the meandered antenna provides an acceptable prediction showing a liner increase in resonant frequency as a function of increasing bending sections, however, in the real case, the resonant frequency of the meander line antenna will not linearly increase with the number of sections [2][3].

The limitation of inductor circuit model of the meandered antenna is still in examining, we simulated that some of the physical properties varied and the corresponding change of the resonant frequency. Firstly, we change the s in M1 configuration from 1cm to 2cm, the resonant frequency behavior of the antenna versus the meandered sections is shown in Figure 2.4. We can observe that the actual resonant frequency will not precisely change as we seen in Figure 2.3.

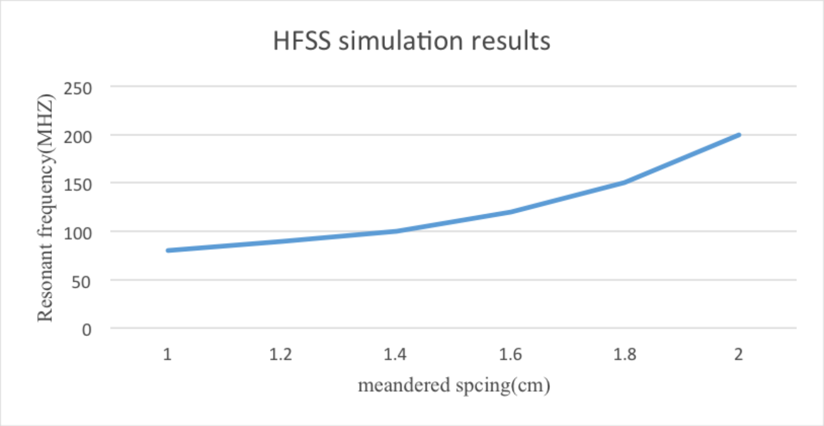

Fig. 2.4: resonant frequency vs meandered spacing

Next, we examined the effect of bending angle changing for each meandered section shown in Figure 2.5 [2]

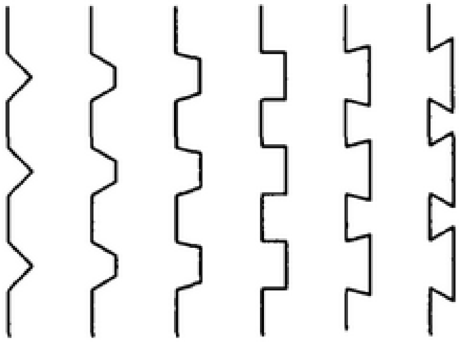

Fig. 2.5: Bending angle when $\alpha=$ 45,60,75,90,120 degree conditions

We bend the antenna for the configuration M5 too see the simulation results in HFSS while keep the total physical length and spacing as the same as the previous model. The relation between bending angle and self-resonant frequency is shown in Figure 2.6 [1].

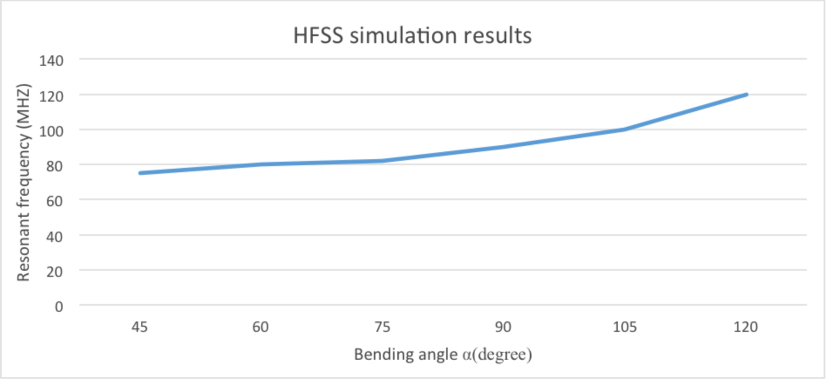

Fig. 2.6: the relation between bending angle and resonant frequency

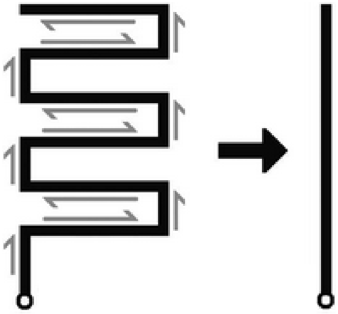

Fig. 2.7: radiation principle of a 90 degree bending meandered antenna

It is observed that resonant frequency would experience a little fluctuate when the bending angle is changing from 45 to 120 degrees. Nevertheless, we need to obtain a relatively large difference between cross-plane and co-plane polarization, as we can see in Figure 2.7, the 90 degree bending angle will provide a cancellation of radiation in horizontal axis due to the opposite flowing direction of two current. At the same time, the radiation current will always along a same direction in vertical axis, as a result, the radiation of the 90 degree bending antenna is equivalent to a single line monopole antenna. Furthermore, the 90 degrees bending method will save room on PCB board so that the total physical length of the antenna will get dropped [1].

2.1.2 Antenna Building and Testing

After investigating the effects of numbers of section, section spacing and bending angle, we start to build a meandered antenna on the substrate to satisfy the specification of the antenna parameters. As seen in Figure 2.8, the spacing between each meandered section is 0.5cm, the number of meandered sections is 14 in total, and the S11 graph is shown in Figure 2.9 which provide us a return loss below -10dB at 80MHz.

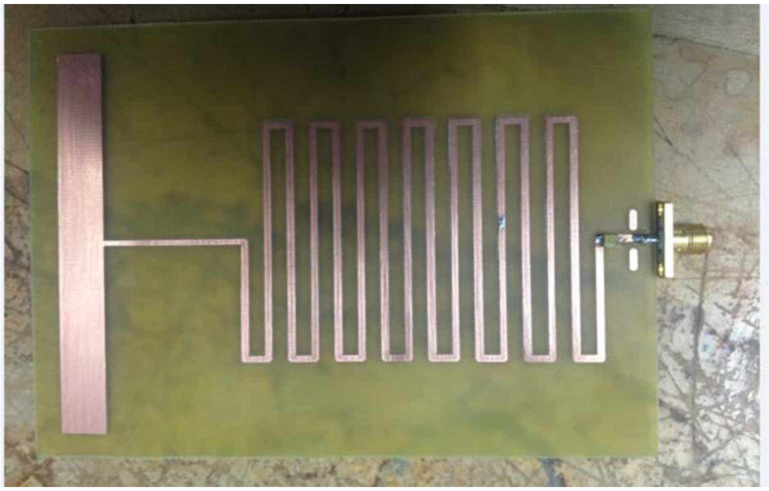

Fig. 2.8: final antenna view

The physical length of this antenna is 80cm in total with the height of 10cm on the substrate, a top loading cap is added at the far end of the antenna to increase the S11 performance. To match up the resonant circuit, we add a 400nH inductor at the feeding point of the antenna. When testing the S12 parameter, we used a $\lambda/4$ dipole antenna as port 2 in HFSS so that the designed antenna is acting as a receiving antenna in the air box. The simulation model is shown in Figure 2.9. And the simulation results are listed in Figures 2.10, 2.11 and 2.12.

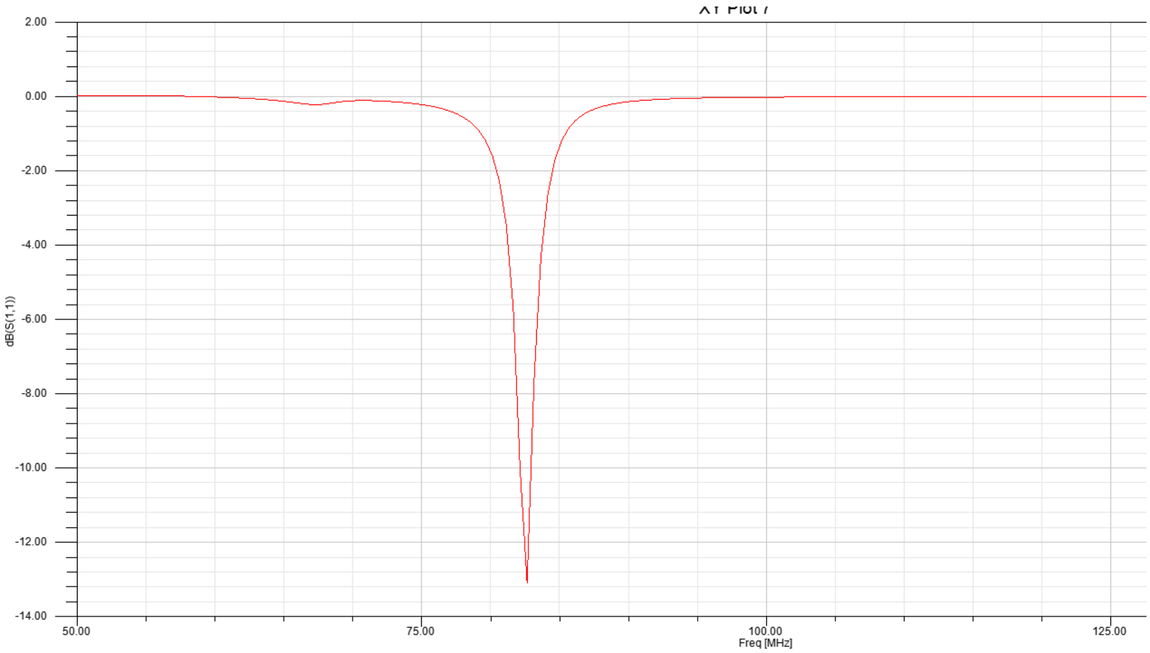

Fig. 2.9: S11 curve for meandered antenna in HFSS

In the real testing, the resonant frequency got shifted to 95MHz due to the inaccurate selection of the inductor value, since we can only get 330nH or 470nH one from the lab, the result frequency will not located in 80MHz.

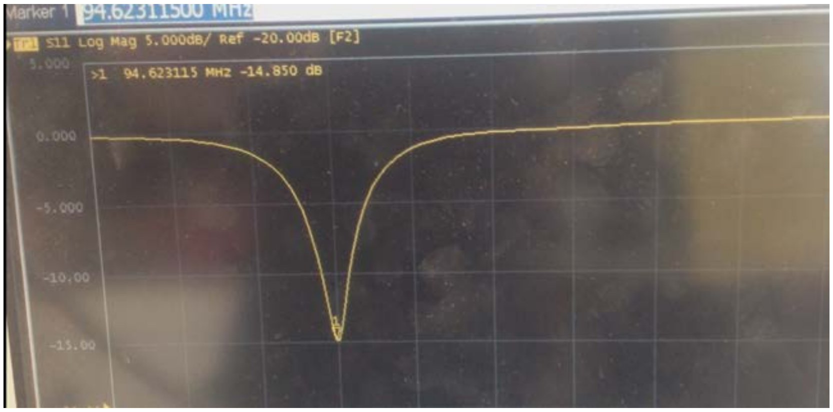

Marker 1 94.62311500 MHz

Tr1 S11 Log Mag 5.000dB/ Ref -20.00dB [F2]

>1 94.623115 MHz -14.850 dB

Fig. 2.10: S11 curve for real testing results

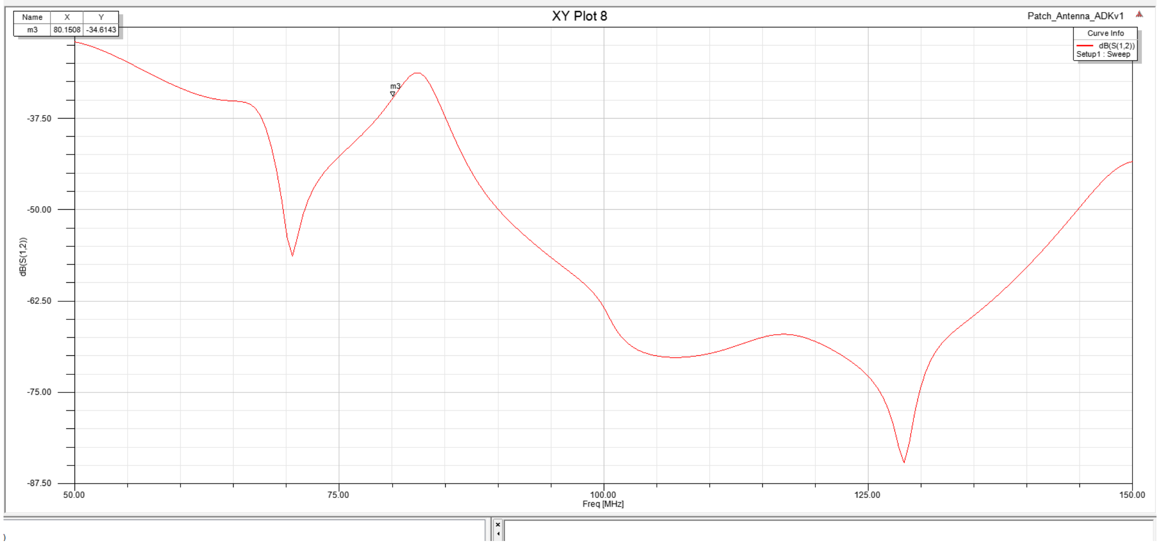

Name	X	Y
m3	80.1508	-34.6143

Fig. 2.11: S12 curve for cross-plane polarization in HFSS

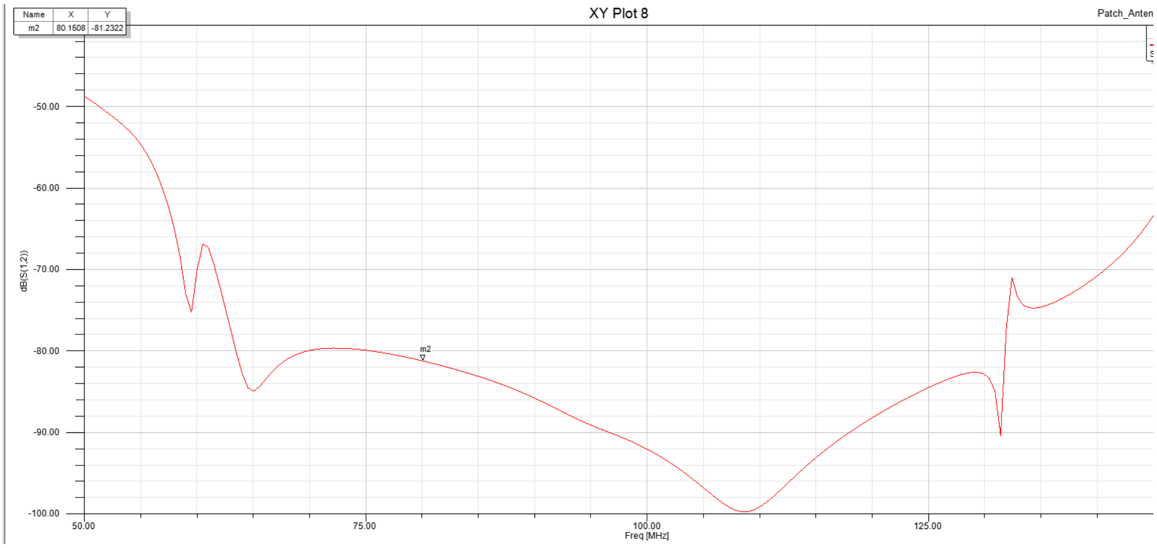

Fig. 2.12: S12 curve for co-plane polarization in HFSS

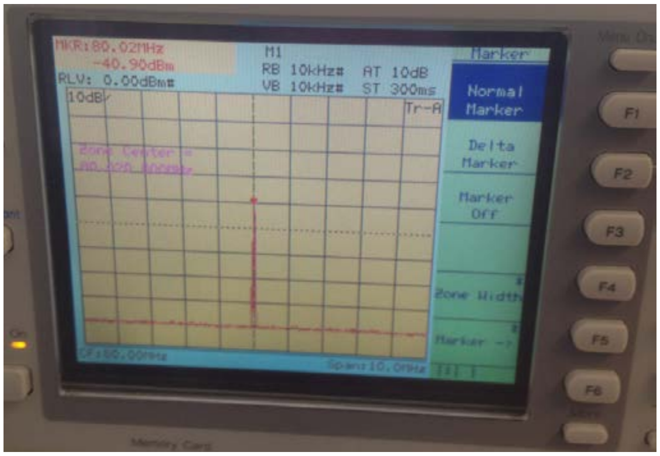

Fig. 2.13: S12 for cross-plane polarization in real test

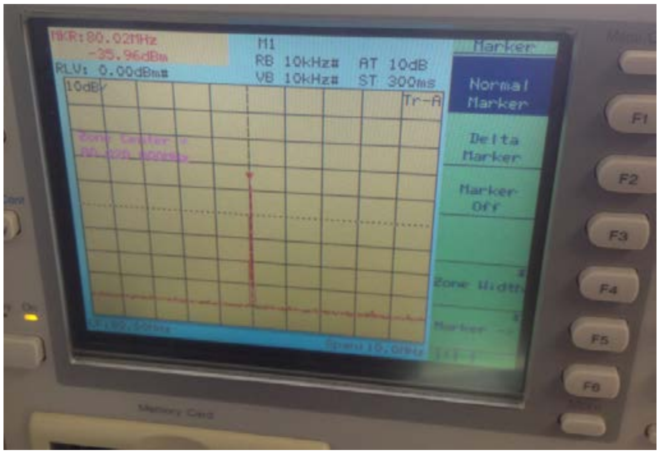

Fig. 2.14: S12 for co-plane polarization in real test

As a conclusion, for S12 curves shown in Figures 2.13 and 2.14, in HFSS the results is pretty good that difference between co-plane and cross-plane of S12 is about 15dB, but in the real test, the difference is 5db, the cause for the difference in quantity is from the non-ideal air box and ground plane from the lab comparing to the ideal ones in HFSS. Further improvement for the testing method is still required.

2.2 H-field Antenna

2.2.1 Purpose

Normally microwave imaging systems consist of a simple E-field antenna such and a monopole or a dipole antenna which has one polarization and it is limited in its functionality, however it is simple to model in the imaging inversion algorithm as these types of antennas have very simple and well defined current distributions along them. Due to a grain storage bin being round, metallic, and closed off at both ends, it can be thought of as a cylindrical resonant chamber which introduces a level of difficulty in designing antennas that can operate in such an environment. However since the walls of the bin are metallic, the field components at the metallic walls are easily differentiable, the H-fields are tangential to the metallic walls of the chamber, and the E-fields are perpendicular to the walls, thus we would like to have an antenna that is capable of probing the tangential H-fields only.

The H- field antenna design had to be confined to the following design criteria in order for it to be effective inside of the grain bin:

1. Ability to pick up H-field only, and reject most of the E-field
2. Minimal size (less that 15cm in length or witdth)
3. Frequency of operation between 70Mhz-90Mhz
4. Matched to 50 ohm coaxial transmission line

5. Physically able to withstand grain being filled into the bin
6. Reduced complexity(for ease of modeling in the inversion algorithm)
7. Ease of manufacturing and reproduction

2.2.2 Research

The typical design procedure for an H-field antenna is a loop of perimeter one λ as at that length the loop becomes purely resistive with the maximum amount of radiation resistance, however this approach does not work for the grain bin as the perimeter of the loop would have to be almost 4 meters.

The other typical approach to designing h-field antennas is to decrease the perimeter of the loop and increase the number of turns which allows for the required size reduction that we are looking for as well as enable it to be matched to a 50ohm coaxial line since the radiation resistance is proportional to the number of turns squared $R_r = (\frac{177NS}{\lambda})^2$, however it is also not feasible for the grain bin since it would not guarantee that the antenna does not pick up the E-field as well, and it would be too complex to model in the imaging software.

2.2.3 Design

In order to satisfy the main requirement of the antenna (1) a shielded and slotted loop antenna was chosen, which is a common type of antenna used in radio.

The ground layer around the conductor which acts as the shielding modifies the electric field distribution inside of the antennas cross sectional area due to the boundary conditions on a PEC, thus reducing its effect on the antenna, this effect is confirmed in the simulation results in section 2.2.6. Since the magnetic field passing through the loop induces a current on both the conductor and the shielding, a slot is cut out in the shield to create a capacitance which introduces a phase shift between the two currents and therefore there is a difference in potential across the load [5].

The second requirement (2) was met by reducing the perimeter of the antenna to $\lambda/20$, how-

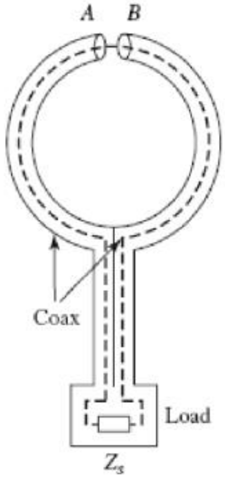

Fig. 2.15: shielded loop antenna [4]

ever the small size presented another challenge which is matching the loop antenna to the 50ohm coaxial line, different ways of matching were considered such as capacitive coupling and transformer coupling between the coaxial line and the antenna, These were simulated in HFSS but found the it would be too complex to build accurately, and it would not be feasible to mount in the grain bin. Mohammad (Project co-supervisor) suggested the use of a 50ohm termination at the end of the loop to match the antenna to a 50ohm line and to cut the loop in half so that the size of it could be further reduced as well as to take advantage of having a metallic wall as the other half of the loop. A prototype of this antenna was built using a semi rigid coaxial cable with a slot cut in the ground conductor and a 50 ohm termination was used to match the antenna to a coaxial line.

A difference of 10db was observed between the E and H polarization. However building multiples of such antennas accurately would not be feasible since the slot size would vary and produce inaccurate results as well as the curvature in the antenna is tough to reproduce accurately.

In order to make the antenna easy to manufacture and reproduce, it was decided that a PCB version would be best suitable.

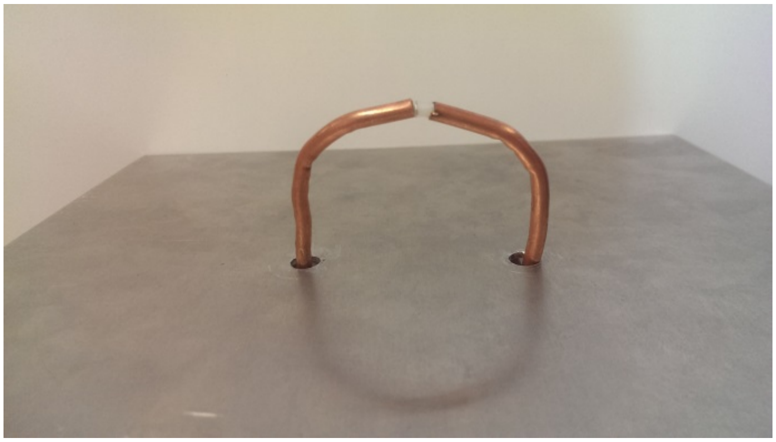

Fig. 2.16: prototype antenna

2.2.4 PCB Antenna Design

To achieve a shielded coaxial line on PCB, a groundless co-planar waveguide was chosen, due to material availability, 0.8mm FR-4 material was chosen as the PCB material with a relative permittivity of 4.3. Due to the limited capabilities of the PCB prototyping machine available at the EIL lab, a minimum cut in the PCB could not exceed 0.2mm, therefore 0.2mm was chosen as the gap between the conductor and the ground planes of the co-planar waveguide. With the help of TX-line (transmission line calculation software) a conductor size of 2.57mm with a gap of 0.2mm and a 0.8mm FR-4 thickness yields the necessary 50ohm transmission line. The size of the antenna is 12.5cm in length and 5.5cm in width with 45 degree bends for reducing reflections, the bent sections are 1cm long.

2.2.5 PCB Antenna Simulation

The PCB version of the antenna is constructed in the high frequency structure simulator with FR-4 as the substrate material, copper material on top of the substrate is simulated as perfect conductor and an infinite ground plane as the antennas backing plate. The design is simulated and optimized to obtain its performance characteristics. From optimization a slot size of 1 mm is chosen in the shielding.

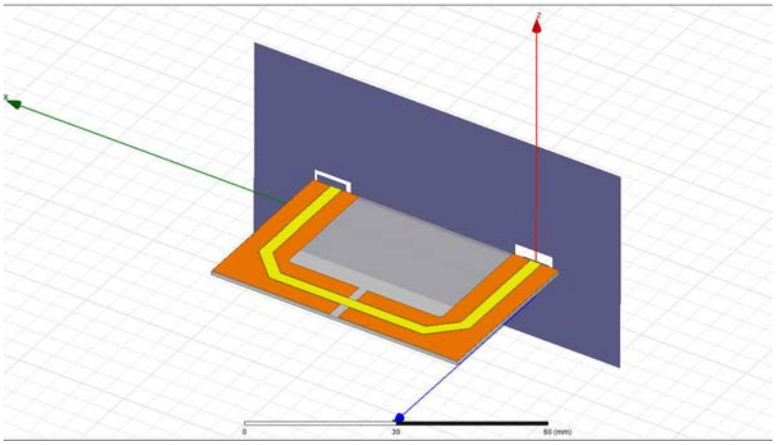

Fig. 2.17: HFSS model of PCB antenna

2.2.6 Simulation Results

The desired result is to have an S11 (insertion loss) of -10db at the frequency of operation, and as expected the insertion loss at 80 MHz is -14.5db as well as due to the 50 ohm termination the antenna has a really high bandwidth.

The simulation also confirms the effect of the co-planar ground plane on the Electric fields inside the cross sectional area of the antenna, Figure 6 and Figure 7 show the antenna with shielding and antenna without shielding E-field magnitude distribution in the cross sectional area.

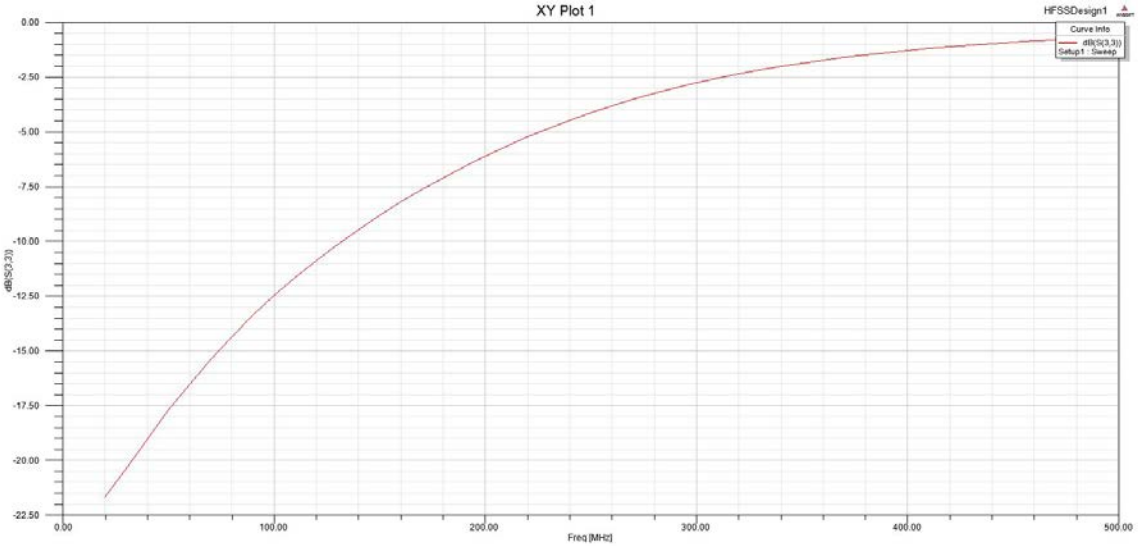

Fig. 2.18: S11 simulated

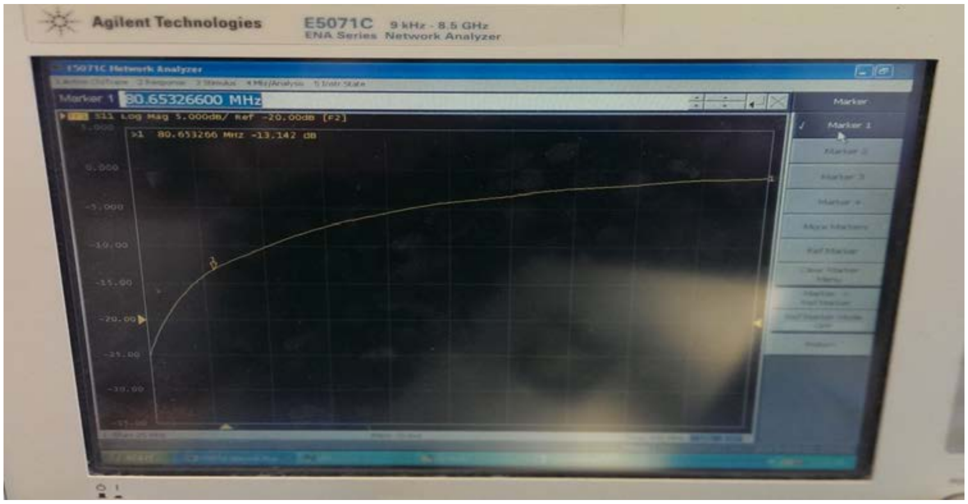

Fig. 2.19: S11 of actual antenna

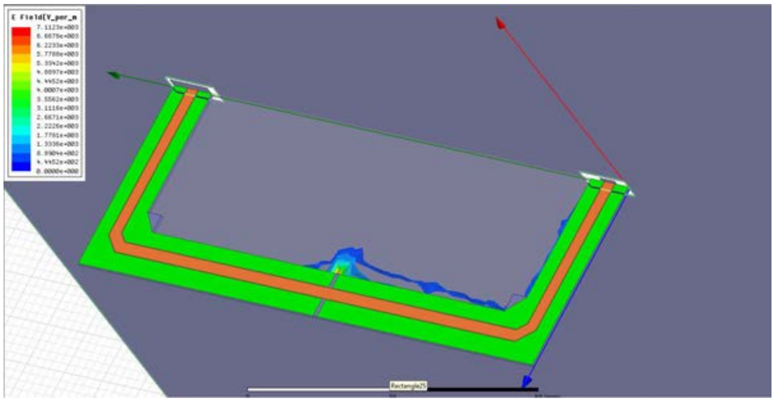

Fig. 2.20: E distribution with shielding

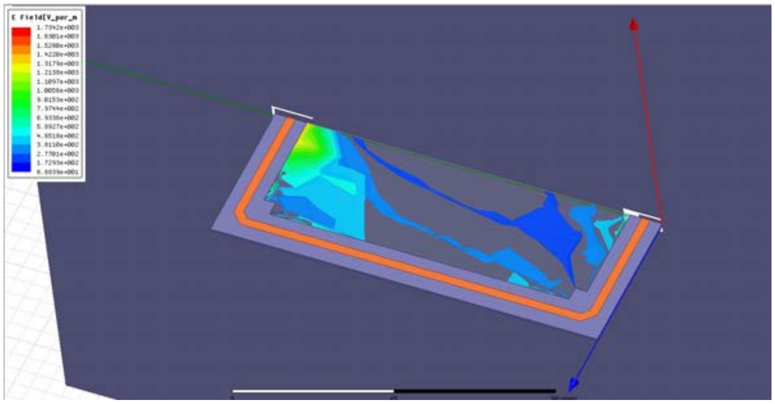

Fig. 2.21: E distribution Shielding removed

2.2.7 PCB Layout

After simulating the antenna in HFSS, the design was transferred to Altium which was used to create the necessary Gerber files for fabrication. The antenna was fabricated in the EIL with the use of the rapid PCB prototyping machine.

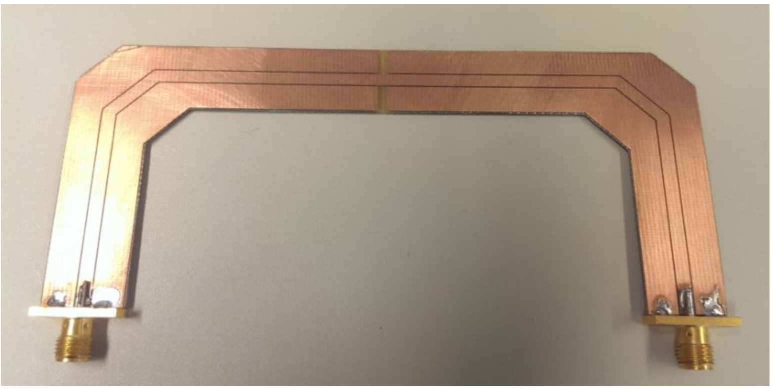

Fig. 2.22: fabricated antenna

2.2.8 H-field Antenna Testing

The antenna's ability to reject the Electric field was tested in a G-TEM cell. The G-TEM cell creates transverse EM waves guided between a pair of plates with H orthogonal to E, the incident wave was created with a signal generator producing an 80 MHz sine wave with 0dbm power and the AUT measurements were taken with a spectrum analyzer. Two orientations of the antenna were tested in the cell, longitudinally parallel with the magnetic field (E-orientation) and perpendicular to magnetic field (H-orientation).

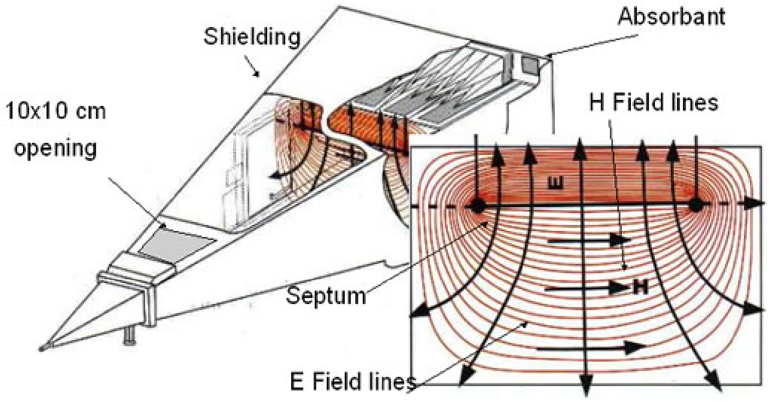

Fig. 2.23: field lines in G-TEM for reference

2.2.9 G-TEM Test Results

The noise floor of the antenna was measured at -83dbm with incident power of -13dbm.

When oriented in the E-orientation the antenna received -81dbm which is close to the noise level of the antenna, when oriented in the H-orientation the antenna received -65dbm therefore a difference of 16db exists between the two orientations which shows that the antenna is picking up only H-field.

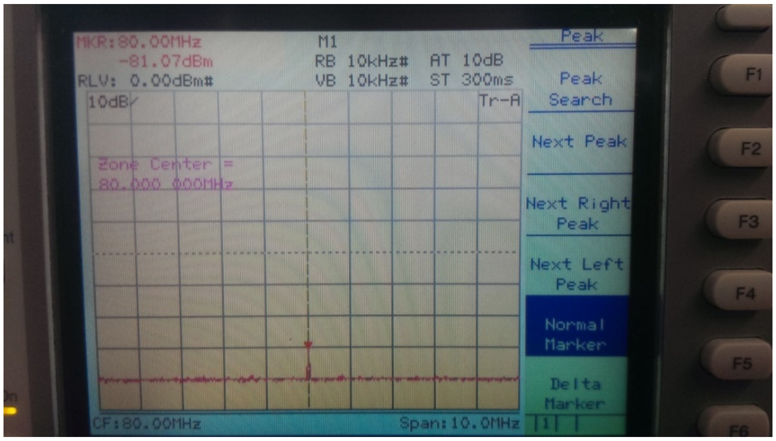

Fig. 2.24: E-orientation

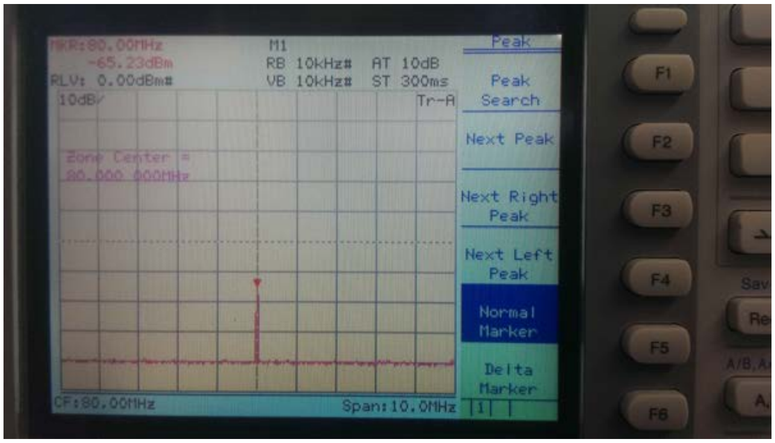
MKR:80.00MHz
-65.23dBm
RLV: 0.00dBm#
M1
RB 10kHz# AT 10dB
VB 10kHz# ST 300ms
10dB/
Tr-A
Zone Center =
80.000 000MHz
CF:80.00MHz
Span:10.0MHz

Fig. 2.25: H-orientation

Chapter 3

Multiplexer

The multiplexer consists of two sections; an RF switch section and a DC switch section. The RF switch provides a path for the signal to and from the VNA to the antennas, while the DC switch provides the logic necessary to set the correct path in the RF switch at the correct time. In order to collect the data required to create an image of the grain bins contents, an array of antennas needs to be connected to the VNA. Figure 3.1 shows how the multiplexer connects the VNA to the array of antennas. The VNA has two ports, one which transmits a signal and one which receives a signal. Through commands sent from the DC switch, the multiplexer is capable of connecting either of these two ports to any of the antennas in the array.

3.1 RF Switch

3.1.1 Background

The multiplexer must connect the ports from the VNA in a certain sequence. First, the multiplexer will be configured to connect the transmitter port from the VNA to antenna 1. After this, antenna 2 will be connected to the receiver port of the VNA. Then antenna 3 connects to the receiver port, then antenna 4 and so on through the entire array of antennas. Once this sequence has been completed the multiplexer will now be configured to connect the transmitter port of the VNA to antenna 2, after which antenna 1 will be connected to the receiver port, then antenna 3, then antenna 4 and so on through the entire array again. The multiplexer will repeat this sequence until all antennas have acted as the transmitter with the remaining antennas acting as receivers.

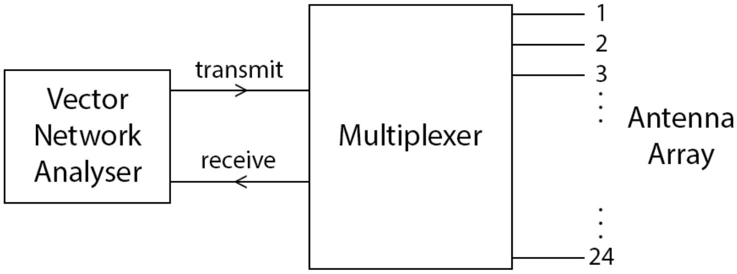

Fig. 3.1: Multiplexer connecting VNA to antenna array

3.1.2 Design

An initial design for the RF multiplexer was created using six 4 x 2 matrix switches together two SP3Ts. The topology of this design is shown in Figure 3.2. Note that not all of the 4 x 2 matrix switches are shown in the Figure, 4 more of these switches are connected to the two remaining pins of the two SP3Ts for a total of 24 antennas. The 4 x 2 matrix switch chosen for this design was from Hittite Microwave Corporation, part number HMC596LP4 and the SP3Ts chosen were part number HMC245QS16 also from Hittite Microwave Corporation. This design was chosen for its simplicity which would allow for good performance.

However, we were not able to use this design, as it was realized that the 4 x 2 matrix switches chosen do not operate in the frequency range needed for our project of 70 - 90 MHz. More research was done but no switches of this type were found that operate in the required frequency range for this project. Due to this limitation a new design was chosen consisting of a series of cascaded RF switches, including SPDTs, SP3Ts and SP8Ts. The topology of this design is shown in Figure 3.3. The switches used in this design are HMC349MS8G, HMC245QS16 and HMC253QS24 from Hittite Microwave Corporation.

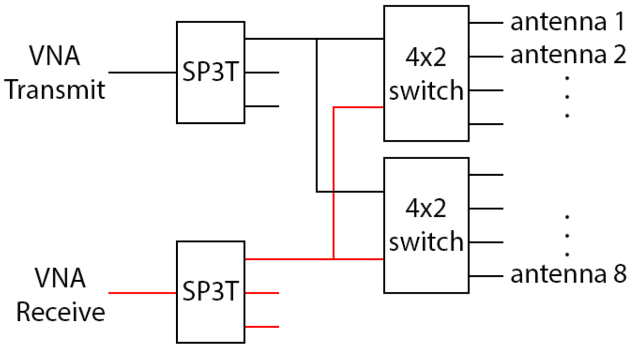

Fig. 3.2: Initial design of the multiplexer

With this design decided on, we needed to get it manufactured on PCB. To create the PCB layout necessary to get these boards printed, software package Altium was used. Two boards were designed for the RF portion of the multiplexer; one containing only an SP3T and one containing two SP8Ts and eight SPDTs. The final 2 x 24 multiplexer requires two of the boards with SP3Ts and three of the boards with SP8Ts and SPDTs. The final PCB layout of the two boards is shown in figures 3.4, 3.5 and 3.6.

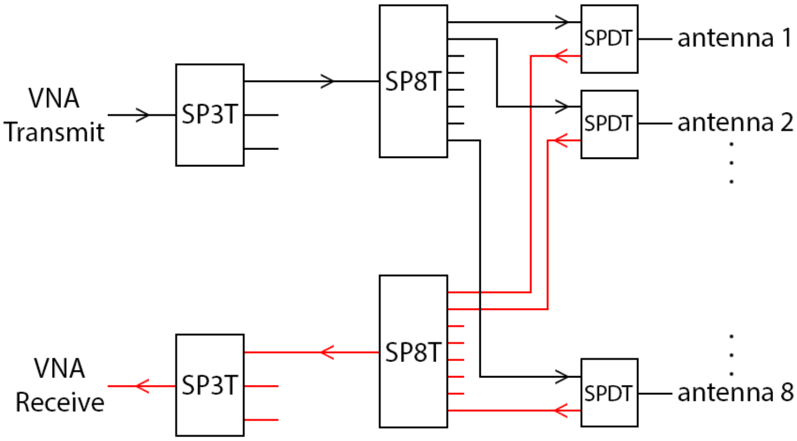

Fig. 3.3: Final design of the multiplexer

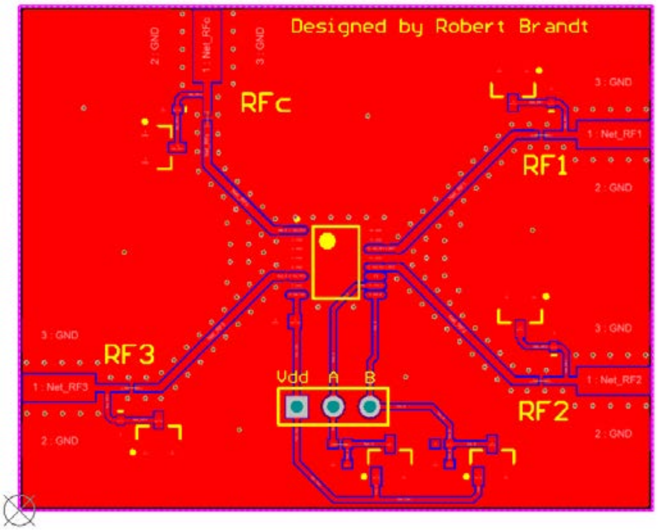

Fig. 3.4: PCB layout for SP3T board

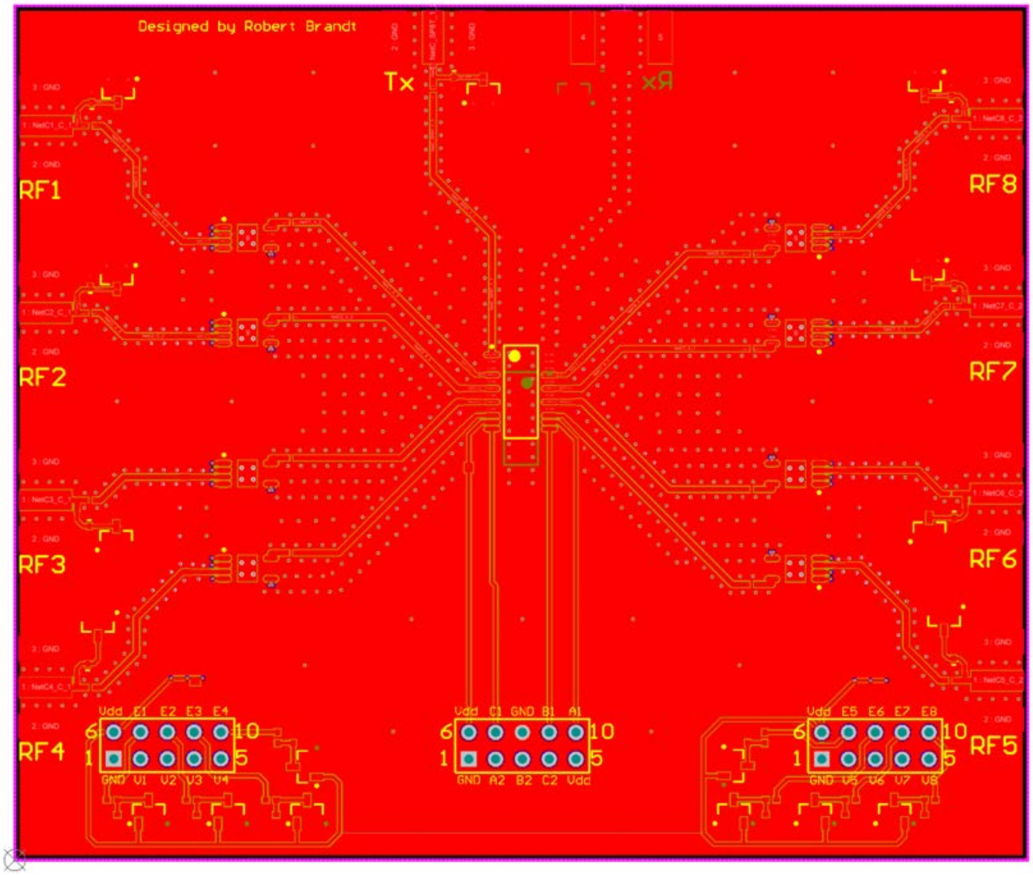

Fig. 3.5: PCB layout for top layer of SP8T and SPDT board

Both boards were designed with 4 layers using a substrate of FR-4. The stack up of the boards consists of a top signal layer, followed by a substrate layer, then an internal signal layer (used only as ground in this design) and then the prepreg layer. Below the prepreg layer is a mirror of what is on top of it; an internal signal layer, then substrate layer and then bottom layer. The stack up from Altium is shown in Figure 3.7.

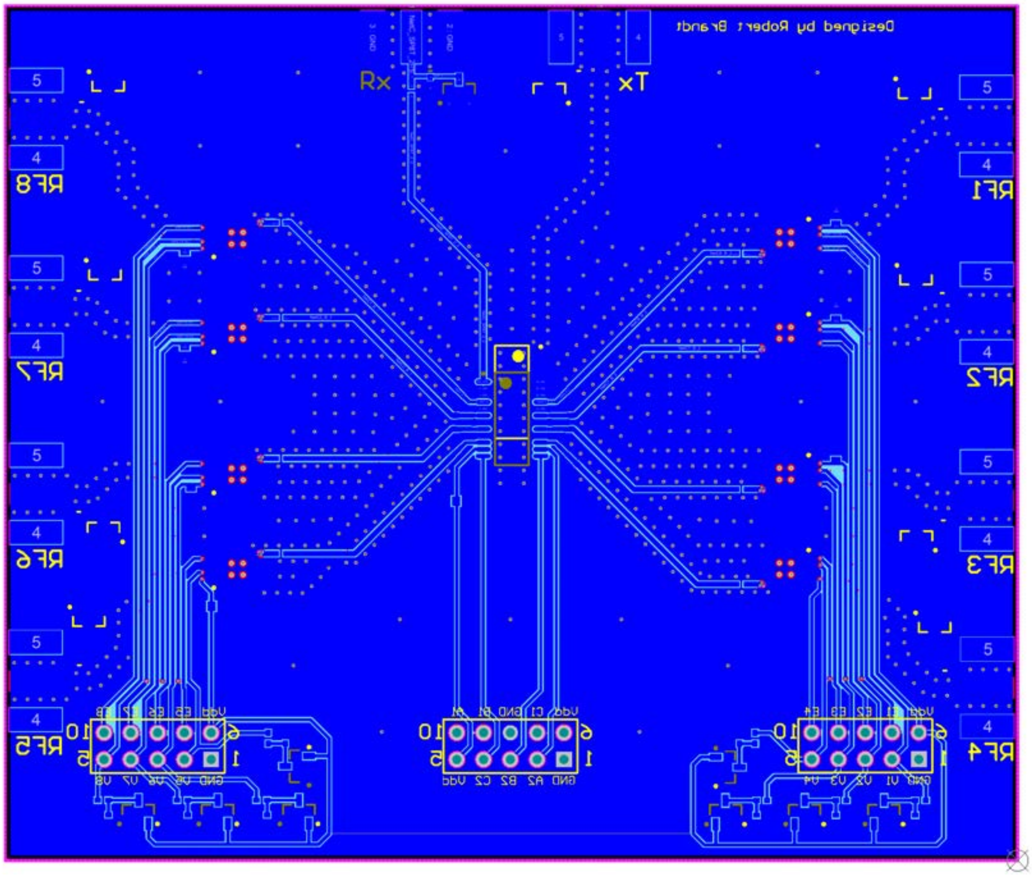

Fig. 3.6: PCB layout for bottom layer of SP8T and SPDT board

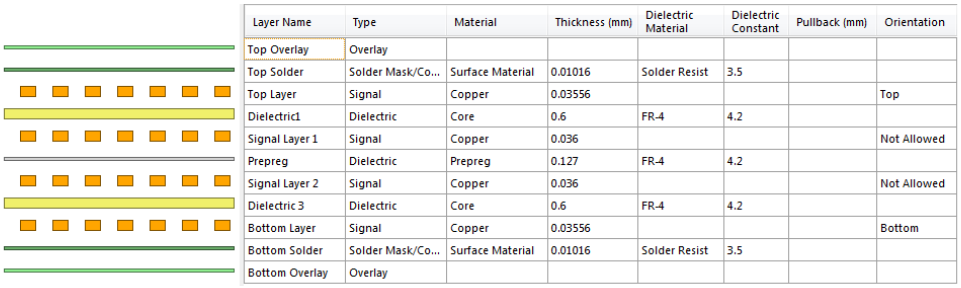

Layer Name	Type	Material	Thickness (mm)	Dielectric Material	Dielectric Constant	Pullback (mm)	Orientation
Top Overlay	Overlay						
Top Solder	Solder Mask/Co...	Surface Material	0.01016	Solder Resist	3.5		
Top Layer	Signal	Copper	0.03556				Top
Dielectric1	Dielectric	Core	0.6	FR-4	4.2		
Signal Layer 1	Signal	Copper	0.036				Not Allowed
Prepreg	Dielectric	Prepreg	0.127	FR-4	4.2		
Signal Layer 2	Signal	Copper	0.036				Not Allowed
Dielectric 3	Dielectric	Core	0.6	FR-4	4.2		
Bottom Layer	Signal	Copper	0.03556				Bottom
Bottom Solder	Solder Mask/Co...	Surface Material	0.01016	Solder Resist	3.5		
Bottom Overlay	Overlay						

Fig. 3.7: Stack up for PCBs in Altium

Both boards used co-planar waveguides with ground for all of the RF traces and were designed such that they were 50 ohms. This resulted in a trace width of 0.5 mm and a gap of 0.115 mm with a substrate thickness of 0.6 mm. Three 10 pin connectors were added to provide power as well as connect all of the control pins for the SP8T and SPDT switches [6].

Unfortunately, due to issues with our original intended supplier of our PCBs, we were unable to get these PCBs printed in time for this report. We found another supplier for our PCBs and hope to have them before our presentation. The PCBs needed to be modified somewhat due to different PCB specifications from this new supplier. Minimum routing size was larger at 0.1524 mm compared to 0.1 mm with the original supplier. Also, the substrate thickness options were different, not allowing us to use a thickness of 0.6 mm. Based on the specifications of the new supplier the RF traces needed to be modified to 0.185 mm thick with a gap of 0.1524 mm. This is based on a substrate thickness of 0.1 mm.

3.2 DC Switching

A DC switch used in combination with and RF switches reduces the total labor and cost of having a separate pathways for each antenna. This therefore enhances the portability of the design and reduces the complexity of very expensive PCBs. due to the cheaper cost in comparison to their RF counterparts and the reduction in frequency interference due to the maximum attenuation of any frequency components at DC. For our design we need a DC circuit for address decoding of the RF switch. In effect, the function of the DC switch is to set the control parameters in order to specify what the response of the RF switch will be at that point in time.

At the onset of the project, we examined the previous switch design to understand how it would integrate with the RF switch and set the control parameters for the acquisition of data by the VNA. Our goal was to improve upon this design so that it was feasible with the new system we wanted to implement.

The design of the switch required the use of Altium and the Arduino user interface. The hardware was designed in Altium and the software was writing in the Arduino mainframe in the C++ programming language

3.2.1 Hardware

The initial design appeared very complex and cumbersome to deduce because it had wires everywhere. The first task was therefore to ascertain the possibility of having a neater hardware with very minimal adjustment to the circuit after the printing of the PCB. This meant that most of the design should be implemented in the PCB in order to reduce complexity and make troubleshooting easier. This also ensure a reduction in noise cause by all the numerous wiring and addition electrical components that was everywhere.

Figure 3.8 highlights that function of the DC switch in perfect simplicity. The control parameters are letters from A to L and these are sourced from the DC switch to the SP3Ts, SP3Ts and SPDTs of the RF switch

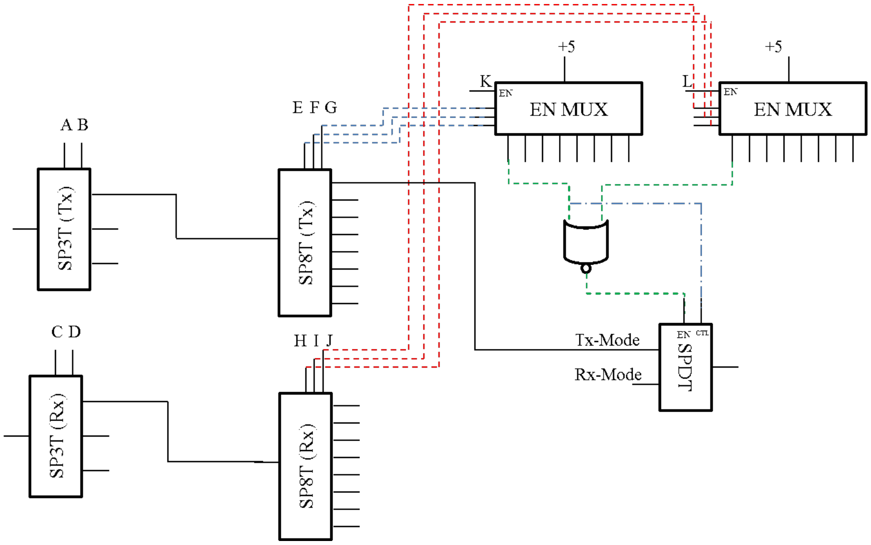

Fig. 3.8: Topology for the integration between DC and RF Switches

Designing the PCB first started with the schematic and a review of the schematic to ensure its accuracy. Figure 3.9 is the initial schematic that was used in the printing of the PCB in Altium. This was designed to be efficient and less complicated however, the simplicity brought about some complication when it was being integrated with the RF Switch.

Using an Arduino board, the previous schematic was put to the test. It proved to work in every sense of the word without any glitches. It carefully selected that right control parameters and turned the respective led pins on which meant theoretically, we had a good hardware and software.

The simplicity of the first designed was questioned when the second version of the RF switch design was completed and had a similar schematic design as the previous design. This implied that the new improvements made to the design, which was based on using a 4x2 matrix switch, was not going to be feasible with the original schematic and a more complex design is shown in Figure 3.10 had to be implemented. It is definitely more rigorous that the first but had however proved to be better. It this sense, the DC switch supports a multilayer RF switch design and can feasible

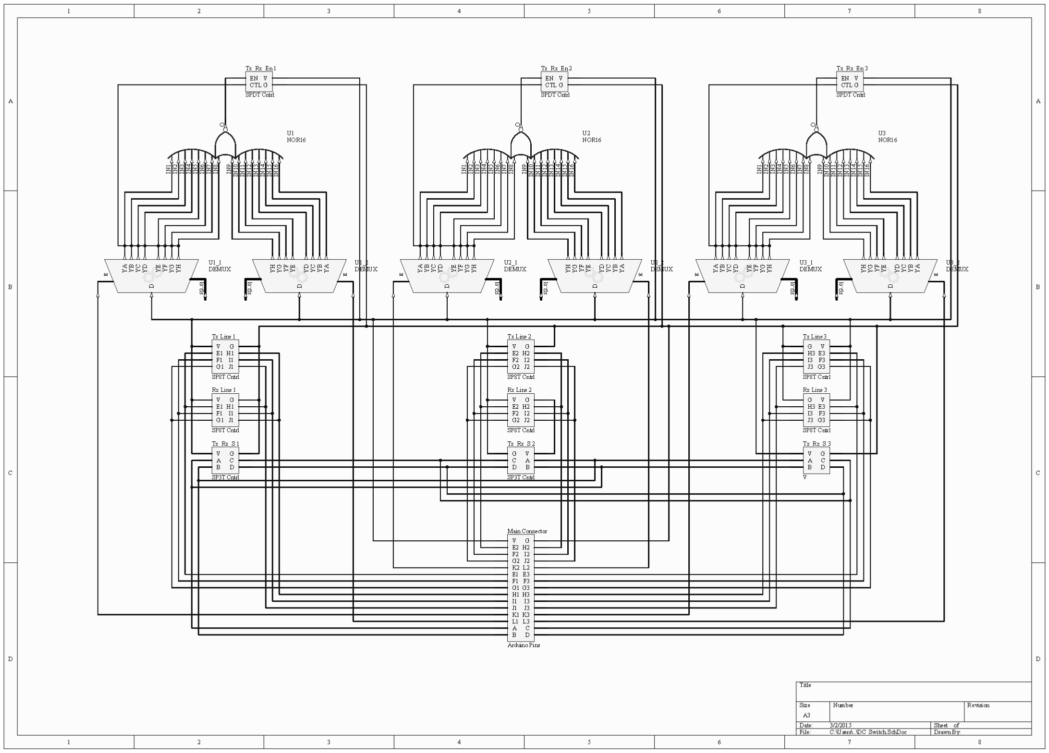

Fig. 3.9: Initial DC Switch Design for Matrix Switch Design

be cascaded with a similar DC switch design should the side of the antennas double or quadruple with the addition of an external enable switch.

Software

The software control of the DC switching circuit is done by an Arduino microcontroller loaded with a table that references the control lines for each multiplexer. This allows the SPDTs to function as an input or an output depending on the values set on the control lines but the Arduino. And will be concurrent with the presents action of the VNA such that, only one SPDT is in transmit mode at a given time. The software will also turn on one the SP8T for transmission of the signal

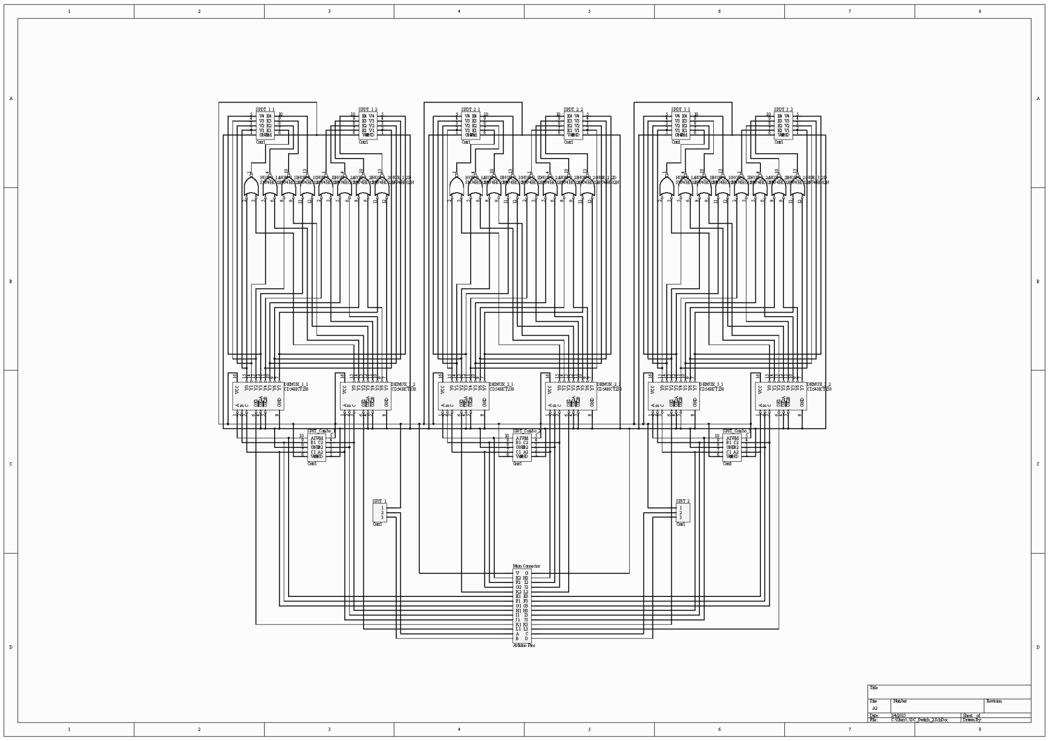

Fig. 3.10: Final DC Switch Design for Multi-Layer RF Switch Design

and turn the other SP8Ts responsible for reception of the signals.

After the research and understanding of requirements were satisfied, a truth table was drawn in order to simplify the circuit to its least possible scenario where the fewest components are used to achieve the expected results. This truth table was then transcribed into code for and then loaded unto the Arduino. This Arduino was set to function in synchronism with the Raspberry Pi.

The pins to be used for the DC circuit had to be chosen in such a way that they match the truth table shown in Appendix D. The Arduino code was then written to first store the truth table in memory and query the table with instructions when needed. The row will be traversed and parameters set according to the value stores in that position of the array referencing an Arduino pin.

This was an improvement on existing software which use a number of arrays to store the information and therefore introduced some time delay when looping through these arrays. The software was loaded unto the Arduino and tested with LED lights to show its effectiveness in selecting the right layer and facilitation the transmission and reception of signals. Our initial design required such a table for address decoding of the switch however, dues to design change, the code was modified to attempt to address decode single pole ICs. The intention was to leave it as a table for future improvements however, with time, it was realized that it made the code slower than expected and could easily pose problems for anyone who was not familiar with using multidimensional tables.

The software was enhanced and improved by first by connecting the Arduino to a breadboard and sending it the initial start instruction. And observing on the board that the right control parameters was being set for the RF switch via the automated Arduino function. The goal of the software side of our project is to get the Raspberry Pi to send a specific number which would correspond to one of the antennas and this will be used for transmission of the signal. This would cause the the Arduino will set the parameters for transmission via that antennae and would be followed by a series of code setting the parameters from the reception of the signal via the remaining twenty-three antennas. Thus after one transmission via serial input, the Arduino would receive twenty-three reflected signals via serial without having to call the send any loops for the receiving signal.

A few scenarios posed during our troubleshooting sessions brought about the need for this more robust code to be written to the Arduino. Firstly, we were going to be use our devices on farm and chances are, the farmers will not have the expertise to trouble shoo when something goes wrong. There were different implementable codes written to address these potential issues. However, the synchronization between the Arduino software and the Raspberry Pi made this almost impossible to accomplish.

It was considered that either the Raspberry software of the Arduino software should be capable of automated function once the start button is push or a signal is sent to a pin in order to make starting the data acquisition and stopping the running routine easily understood to the average farmer.

3.2.2 ESD Protection

Any reliable system design requires some form of Electrostatic Discharge protection. Choosing the right circuit protection device involves considering criteria such as: Response time, ESD current handling capacity and, maximum reverse leakage current. Also the device should not interfere with the normal operation of the circuit. Designing the DC circuit also meant taking the RF circuit into consideration in order to minimize electrostatic discharge and current leakage.

We considered N-well resisters, gate-grounded and gate-coupled protection options, silicon controlled rectifiers and diodes. Ultimately we decided to use diodes and capacitors due to its simplicity.

During our design phase, the options available were to implement ESD protection on the antenna or on the switch box. We chose to go with ESD protection for the switch box because it was less expensive to do it that was and it was a trusted and proven route to for to ensure that a great amount of ESD is dealt with in our circuit.

There is no addition intended for the ESD protection. The data sheet and simulations we run serves to hold that our diodes will work well within our range of interest

Chapter 4

Vector Network Analyzer

The vector network analyzer is a key component of the S-Parameter Data Acquisition (SPDAQ) system since it is the actual instrument that measures the S-Parameters of the grain storage unit.

4.1 Harware Specifications

In order to implement a practical system that would be ideally used by agriculturalists such as farmers, the VNA had to be portable yet affordable. Lab quality VNAs are very expensive, usually costing tens of thousands of dollars, and therefore cannot be used for the SPDAQ system. Due to the fairly low frequencies being transmitted and received from the antennas within the grain storage unit, the VNA can be more affordable than those usually found in a lab. On top of these main specifications of a compact, low-costing VNA, the analyzer had to be a two port system so it is capable of S11 and S12 measurements for the microwave imaging of the grain bin,as well as being capable of measuring within the frequency range of a typical grain bin,and can offer a good dynamic range. Table 4.I shows the exact specifications required for the SPDAQ system to be effective.

Table 4.I: VNA Requirements [7]

Frequency Range	70 MHz - 100 MHz
Dynamic Range	10 dB
System Type	2-port with S11 and S12
Budget	<$1000

These criteria help facilitate in the decision of selecting the MiniVNA Pro (MVP) by Mini Radio Solutions which offers a more affordable and portable solution for the VNA component of the SPDAQ system.

Table 4.II: miniVNA PRO Specifications

Frequency Range	0.1 MHz - 200 MHz
Dynamic Range	90 dB in Transmission mode 50 dB in Reflection mode
System Type	2-port with S11 and S12
Cost	$549.95 + taxes and fees

As shown in Table 4.II, the MVP meets all the main VNA requirements for the SPDAQ system which made it a valid solution for the VNA component.

4.2 Calibration and Testing

To ensure that the MVP meets our system's standards, results measured from the MVP were compared to the more high-tech VNAs in the Electromagnetic Imaging Lab (EIL) that are normally used for the imaging data. The MVP is first calibrated using the calibration tool provided by the EIL and calibration files are created using the MVP software, which is shown in Figure 4.1.

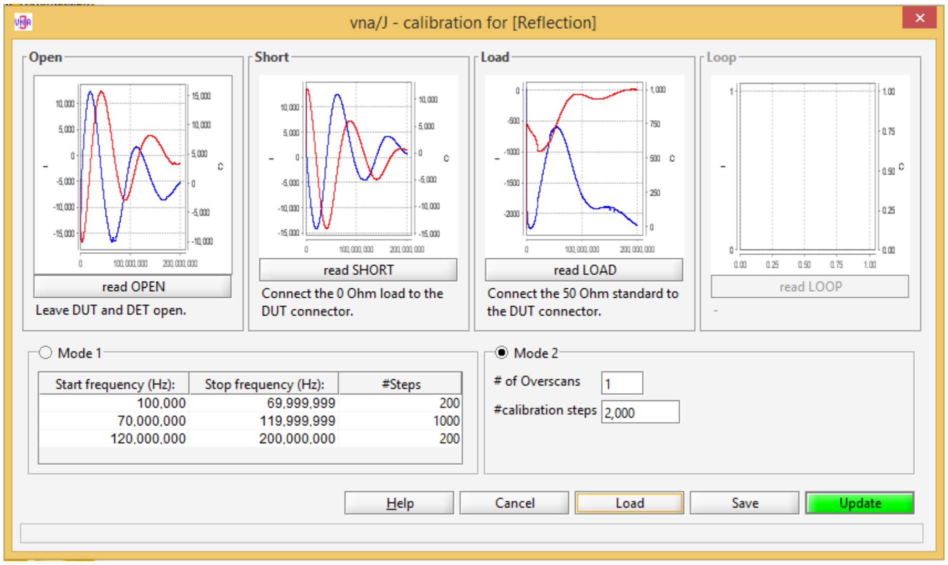

Leave DUT and DET open.

Connect the 0 Ohm load to the DUT connector.

Connect the 50 Ohm standard to the DUT connector.

○ Mode 1

Start frequency (Hz):	Stop frequency (Hz):	#Steps
100,000	69,999,999	200
70,000,000	119,999,999	1000
120,000,000	200,000,000	200

● Mode 2

# of Overscans 1

#calibration steps 2,000

Fig. 4.1: miniVNA PRO calibration software.

The S11 measurement of the miniVNA PRO was then compared to the S11 measurement of the EIL VNA in order to verify the calibration was performed correctly on the miniVNA PRO. The RF Switch module provided by the EIL was used as a load. The S11 output of the RF Switch transfer function is shown in Figure 4.2 and 4.3 for both the EIL VNA and the miniVNA PRO. Both the real and imaginary part of the S11 measurement are fairly similar with a slight discrepancy in the real part of S11 in the miniVNA PRO which may be due to the calibration kit used with the miniVNA Pro since the kit was designed for the EIL VNAs. With fairly accurate results, the MVP gave us confidence in using it for the SPDAQ system.

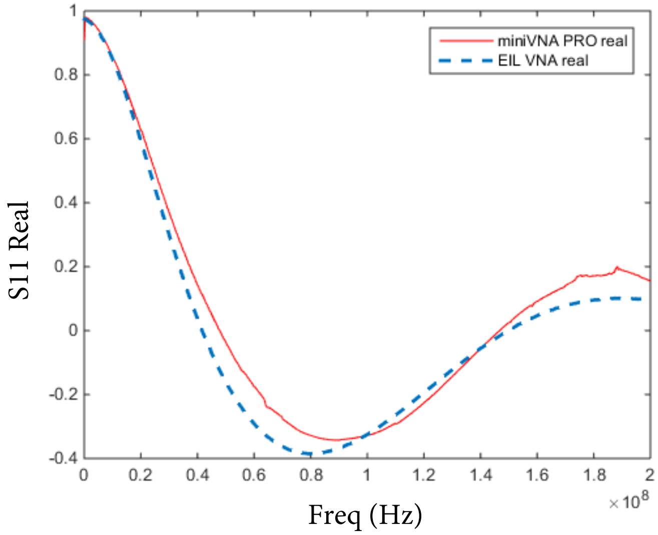

Fig. 4.2: S11 measurement(real) for both VNAS.

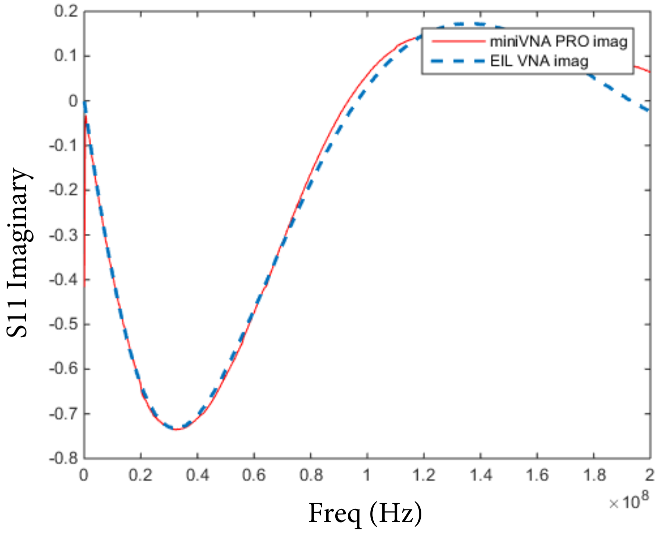

Fig. 4.3: miniVNA PRO open port measurement in reflection mode.

4.3 miniVNA PRO Software

The MVP was designed to be software-defined and the manufacturer did not have any indications that they will make this device open source. This forced our team to go ahead with the manufacturer's software in order to use the MVP despite the slow read times of each measurement.

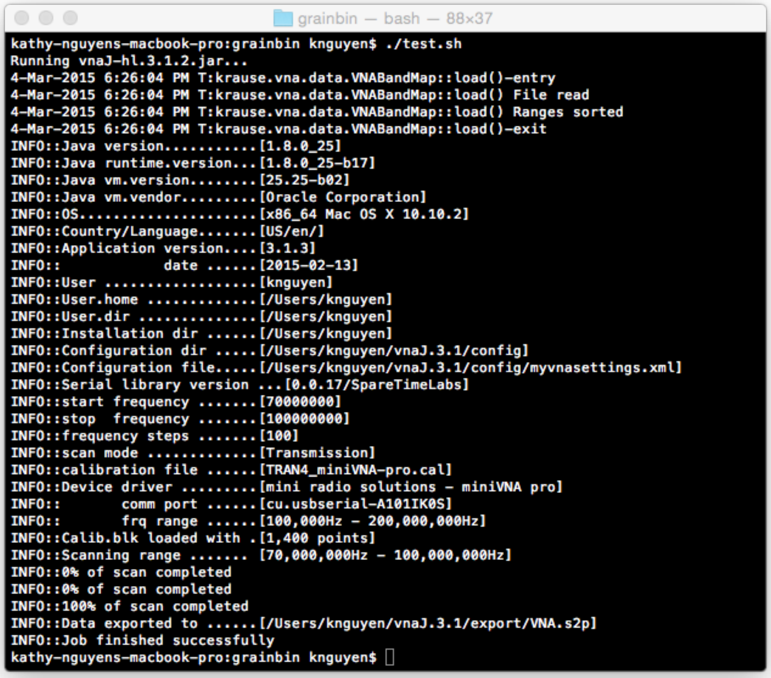

```
kathy-nguyens-macbook-pro:grainbin knguyen$ ./test.sh
Running vnaJ-hl.3.1.2.jar...
4-Mar-2015 6:26:04 PM T:krause.vna.data.VNABandMap::load()-entry
4-Mar-2015 6:26:04 PM T:krause.vna.data.VNABandMap::load() File read
4-Mar-2015 6:26:04 PM T:krause.vna.data.VNABandMap::load() Ranges sorted
4-Mar-2015 6:26:04 PM T:krause.vna.data.VNABandMap::load()-exit
INFO::Java version...........[1.8.0_25]
INFO::Java runtime.version...[1.8.0_25-b17]
INFO::Java vm.version........[25.25-b02]
INFO::Java vm.vendor.........[Oracle Corporation]
INFO::OS.....................[x86_64 Mac OS X 10.10.2]
INFO::Country/Language.......[US/en/]
INFO::Application version....[3.1.3]
INFO::            date ......[2015-02-13]
INFO::User ..................[knguyen]
INFO::User.home .............[/Users/knguyen]
INFO::User.dir ..............[/Users/knguyen]
INFO::Installation dir ......[/Users/knguyen]
INFO::Configuration dir .....[/Users/knguyen/vnaJ.3.1/config]
INFO::Configuration file.....[/Users/knguyen/vnaJ.3.1/config/myvnasettings.xml]
INFO::Serial library version ...[0.0.17/SpareTimeLabs]
INFO::start frequency .......[70000000]
INFO::stop  frequency .......[100000000]
INFO::frequency steps .......[100]
INFO::scan mode .............[Transmission]
INFO::calibration file ......[TRAN4_miniVNA-pro.cal]
INFO::Device driver .........[mini radio solutions - miniVNA pro]
INFO::       comm port ......[cu.usbserial-A101IK0S]
INFO::       frq range ......[100,000Hz - 200,000,000Hz]
INFO::Calib.blk loaded with .[1,400 points]
INFO::Scanning range ....... [70,000,000Hz - 100,000,000Hz]
INFO::0% of scan completed
INFO::0% of scan completed
INFO::100% of scan completed
INFO::Data exported to ......[/Users/knguyen/vnaJ.3.1/export/VNA.s2p]
INFO::Job finished successfully
kathy-nguyens-macbook-pro:grainbin knguyen$ 
```

Fig. 4.4: miniVNA PRO Software Output

The MVPs software used for the SPDAQ system is the 'vnaJ-hl.3.1.3.jar file [9] that runs on a headless system (no graphical user interface). When the jar file is executed with the specified parameters (frequency start, stop and steps), the MVP takes the readings and exports them to a CSV file (the file type is specified within the parameters of the jar file). An example output of the MVPs software running through a command line interface (CLI) is shown in Figure 4.4.

Chapter 5

Microprocessor

5.1 Hardware Integration

Due to the software limitation of the MiniVNA Pro (MVP), a microprocessor was required to run the MVPs software. This is where the Raspberry Pi 2 (RPi2) was chosen. The RPi2 microprocessor will be used to control both the RF Multiplexer and MiniVNA Pro (MVP) of the S-Parameter Data Acquisition (SPDAQ) system. The specifications of the RPi2 are shown in Table 5.I.

Table 5.I: Raspberry Pi 2 Specifications [8]

Processor	900Mhz quad-core ARM Cortex-A7 CPU
RAM	1GB
USB Ports	4
GPIO Pins	40

The RPi2 offers enough USB ports to connect the RF Multiplexer (RF Mux) and MVP. As well, the RPi2 offers GPIO pins, which will be used to integrate user interface (UI) features for the user to have better control of the system. Such UI features that were implemented with the RPi2 was a button to run the SPDAQs software when pressed and a LED indicator to allow the user to know when the program is ready for the user to press the button. A circuit is shown in Figure

5.1 that displays the button and LED connection to the appropriate GPIO pins on the RPi2 (see Appendix C for Raspberry Pi 2 Pinout Configuration).

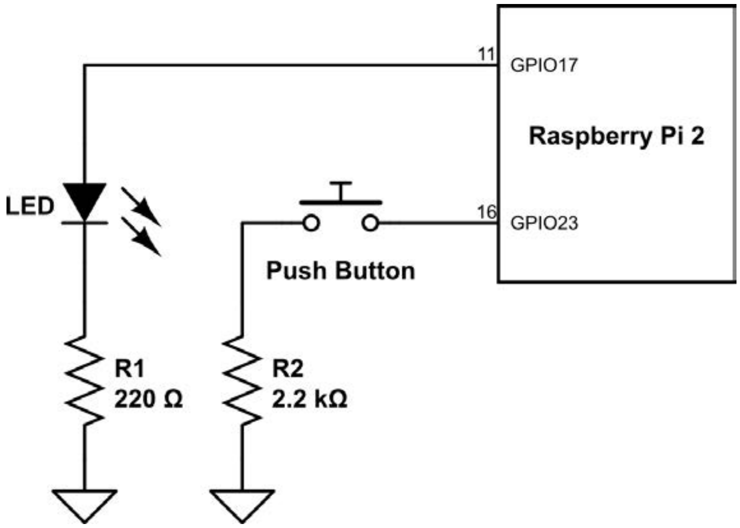

Fig. 5.1: LED and Button Circuit

Initially, the SPDAQ system was designed around the Raspberry Pi Model B+ but due to the new release of the RPi2 in February, 2015, the decision to upgrade seem obvious with the faster processor at the same low cost of $39.99 CAD + shipping that the old Raspberry Pi Model B+ was priced at. The hardware upgrade helped greatly improve the software run times down to 16s per measurement to 5s per measurement. Boot up times for the system also greatly reduced to 6s from 15s.

5.2 Software Design and Integration

Arch Linux was installed onto the RPi2 due to its minimal architecture. It is a lightweight operating system (OS) that is text-based with no GUI making it very quick to boot up. Since the SPDAQ system has no need for a GUI and the software that will be running on the RPi2 did not require much to run, the Arch Linux OS provided a great solution for our system.

For the SPDAQ system, there are four main processes that the system is required to run: Initialization, Data Acquisition, Post-Data Processing, and Remote Data Accessing. The order of all these processes and procedures that run on the microprocessor are shown in Figure 5.2.

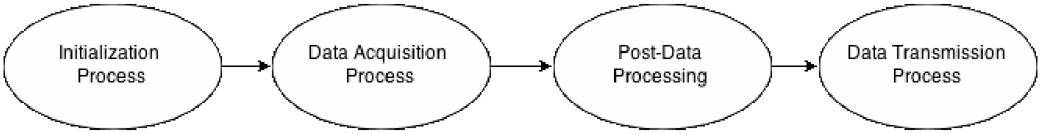

Fig. 5.2: S-Parameter Data Acquisition system processes.

5.2.1 Initialization Process

The initialization process requires the user to interact with the system to power on and start the other processes that are executed by a shell script. The procedure is as follows:

1. Power on the S-Parameter Data Acquisition (SPDAQ) system by connecting the RPi2 to a power source.
2. Once booted up (allow approximately 7s), the user can now press the push button to execute a shell script that will start the data acquisition process.

5.2.2 Data Acquisition Process

In this process, the RPi2 will control both the RF Multiplexer to switch the antennas between transmitter and receiver as well triggering the MVP to execute a sweep to obtain S-Parameters of the Grain Bin. The Data Acquisition Process runs through an N-number antenna array collecting the S-parameter data from the grain bin through the use of the MVP, which exports a CSV file per sweep. Each antenna will act as a transmitter and will loop through all n number of antennas acting as a receiver, which results in an N x N number of measurements. This will also result in N x N number of exported data files from the MVP due to its software limitations. These data files are exported to /root/vnaJ.3.1.3/export directory of the RPi2. A flow chart of the Data Acquisition Process is shown in Figure 5.3 which outlines this procedure.

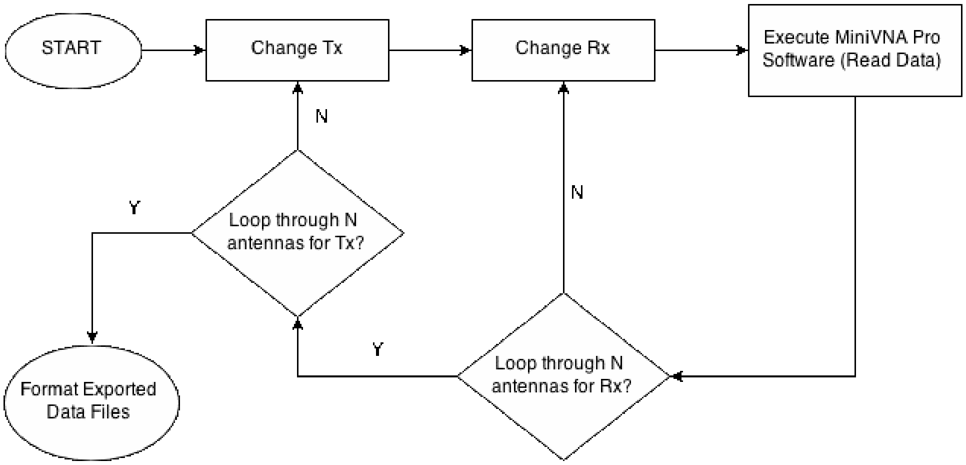
START
Change Tx
Change Rx
Execute MiniVNA Pro Software (Read Data)
N
Y
Loop through N antennas for Tx?
N
Y
Loop through N antennas for Rx?
Format Exported Data Files

Fig. 5.3: Flow chart of the Data Acquisition Process.

5.2.3 Post-Data Processing

Post-Data Processing procedure is executed by the shell script after the Data Acquisition Process is done. In this process, the exported CSV files from the MVP are reformatted to a single data file, which the user can access for further processing such as microwave imaging analysis of the grain bin. The exported CSV files are located in the /root/vnaJ.3.1/export directory with the filename format of

`gbin_(tx)(rx).csv`

where "(tx)" and "(rx)" are the 2-digit transmitter and receiver antenna number, respectively, within the array that the MVP measured from. The MVP exports the data as transmission loss in dB and transmission phase (degrees), which is S12 in polar form, however Cartesian complex form is required for post-analysis and therefore a small calculation is required prior to writing to file. The calculations performed are described below: The MVP provides its data as so,

$TransmissionLoss(TL) = 20\log_{10}|S12|$

$TransmissionPhase = \theta$

The desired data form is as so, $S12 = a + bi$

Variables a and b are calculated as shown,

$a = |S12|\cos\theta$

$b = |S12|\sin\theta$

$where, |S12| = 10^{(TL/20)}$

Once the S12 data is calculated to Cartesian complex format, it is then written to a file called sp.dat which is located in /root/grainbin/output/ directory. The format of the file is shown as:

```
Tx Rx Probe     S12 Real S12 Imaginary (repeating for all frequency steps)
```

Where Tx is the transmitter antenna number and Rx is the receiver antenna number, which is then followed by the S12 real and imaginary data in succession for all 100 frequency steps. A flow chart of the Post-Data Processing procedure is shown in Figure 5.4.

5.2.4 Data Transmission Process

The sp.dat file contains all of the S-parameters of the grain storage unit and this file will be accessible to the user through the cloud if an Internet connection is present. The shell script will execute the data upload process after the Post-Data Processing is complete in which it executes a command in Linux that triggers an upload of the specific file to Dropbox.

Dropbox is a widely used cloud storage service that anyone can register for free for basic cloud storage space. This service can be accessed online remotely from the users own PC through the many interfaces that Dropbox offers (ex. website, computer software, etc.), which makes it very convenient for the user to retrieve the data from the SPDAQ device and therefore was selected for our system. Appendix B.4 instructs how a user can unlink or link a specific Dropbox account onto the RPi2 as well as additional commands.

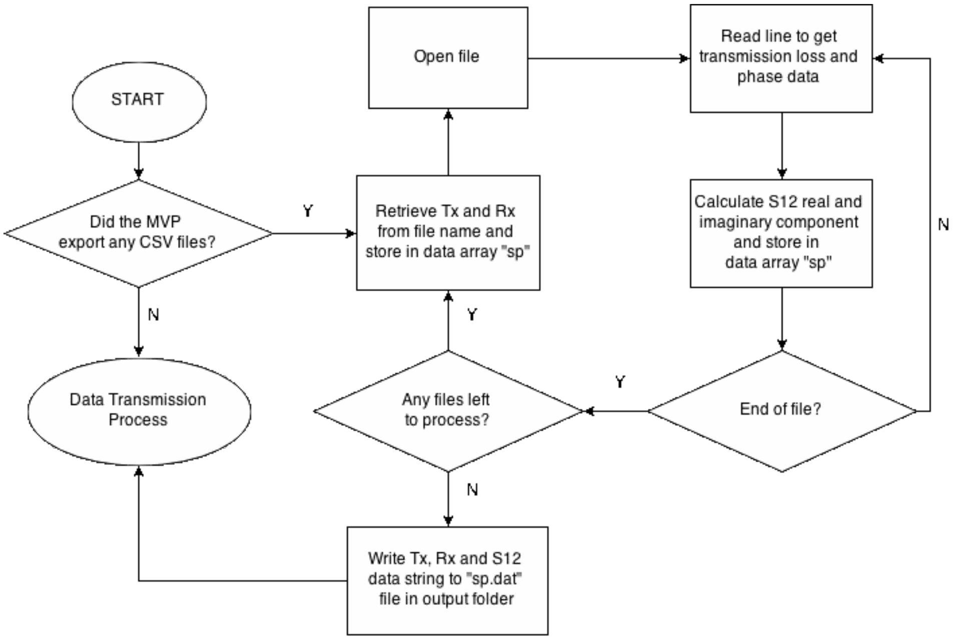
START
Did the MVP export any CSV files?
Y
N
Retrieve Tx and Rx from file name and store in data array "sp"
Open file
Read line to get transmission loss and phase data
Calculate S12 real and imaginary component and store in data array "sp"
End of file?
Y
N
Any files left to process?
Y
N
Write Tx, Rx and S12 data string to "sp.dat" file in output folder
Data Transmission Process

Fig. 5.4: Flow Chart of Post-Data Processing Procedure.

However, if the SPDAQ system is unable to connect to the Internet to upload the data file, the user can still manually retrieve the data through the following methods:

1. Ejecting the micro-SD card located underneath the RPi2 in which the file is stored on.
2. SFTP with the RPi2 through an Ethernet connection with another device.
    - The RPi2 is assigned a static IP address for the user to SSH and SFTP in order to communicate with it. That static IP address is: *192.168.2.23*. Once SFTP establishes a connection, executing the command, *get /root/grainbin/output/sp.dat* will transfer the file over to the users remote device.

5.3 Software Setup and Configuration

This chapter section details the software setup and configuration on the RPi2 to run the SPDAQ software. The purpose of this section is to help a user recreate the SPDAQ software on the RPi2 in the case of any software error or corruption or to simply modify specific software parameters to tailor to the user's needs.

5.3.1 Prerequisites

The RPi2 is setup with a username and password. The default login information for Arch Linux is the following:

```
Username: root

Password: root
```

However for security purposes, the password was changed to 'gbin2015' with the same username. In order for the RPi2 software processes to function, certain files need to be included on the RPi2 stored in the directory /root/grainbin. A list of these files is shown in Table 5.II

Table 5.II: Required files in the /root/grainbin directory of the Raspberry Pi 2.

File	**Description**
vnaJ-hl.3.1.3.jar	miniVNA PRO headless software
gbin.sh	shell script t run all of the SPDAQ processes (see Appendix B.1)
dropbox-uploader.sh	Dropbox shell script to upload "sp.dat" file to a linked Dropbox account on the RPi2 (see Appendix B.4)
put2str.exe	processes the exported CSV files from the miniVNA PRO (see Appendix B.2)
button.py	button and LED function on the Raspberry Pi 2 (see Appendix C)

Specific packages also need to be installed onto the RPi2 for the files to run properly on the Arch Linux OS. The following commands shown in Table 5.III can be executed on the RPi2 terminal with Arch Linux installed. Ensure that the RPi2 is connected to the Internet in order to download these packages.

Once the packages are installed, the MVP's software requires specific directories to be created. These directories are created when the 'vnaJ-hl.3.1.3.jar file is executed for the first time which can

Table 5.III: Required packages to be installed on Arch Linux OS running on the Raspberry Pi 2.

Command	**Description**
pacman S jdk7-openjdk	Java package
pacman S mono	C# Compiler
pacman S python-raspberry-gpio	Raspberry Pi GPIO Python library

be executed using the following command:

```
java Dconfigfile=gbin.xml -Dfstart=70000000 -Dfstop=100000000 -Dfsteps=100 -Dcalfile=gbin.cal -Dscanmode=TRAN -Dexports=csv -jar vnaJ-hl.3.1.3.jar
```

An error will occur due to certain files missing when the command is executed for the first time however the necessary directories will be created on the /root directory of the RPi2 which includes:

- /root/vnaJ.3.1/export
- /root/vnaJ.3.1/calibration
- /root/vnaJ.3.1/config

There are two key files that need to be present for the 'vnaJ-hl.3.1.3.jar file to execute properly. The first one is the configuration file "gbin.xml" (refer to the vnaJ software manual on how to create this file [9]). The XML file includes the USB port name for the software to communicate with the MVP. This file must be stored in the /root/vnaJ.3.1/config directory. The second key file is the calibration file for transmission mode which are created using the 'vnaJ.3.1.3.jar GUI software that must be run on a separate computer that supports either Mac OS or Windows. The user should consult the vnaJ software user manual [9] for details on how these calibration files are created using the 'vnaJ.3.1.3.jar GUI. This calibration file is stored in the */root/vnaJ.3.1/config* directory.

The RPi2 is now setup to run the 'gbin.sh' shell script that runs the SPDAQ software. In order to use the button and LED feature, the python script 'button.py' needs to be executed. The simple command "Python button.py" will run the python script and will listen for the user to press a button to initiate the 'gbin.sh script. In order to setup the python script 'button.py at bootup, the following command can be entered on the terminal of the RPi2:

```
crontab e
```

A file will come up and in this file enter in the line at the very bottom:

```
@reboot python /root/grainbin/button.py
```

Save the file and now the RPi2 will run the python script at bootup, enabling the button and LED function. To connect the LED and push button to the RPi2, review Figure 5.1 and Appendix C for GPIO pinout on the RPi2.

5.3.2 Configuration Parameters

'gbin.sh Parameters

The 'gbin.sh' shell script file is designed to take four parameters that define the number of transmitters and receivers being used with the SPDAQ system. The command to run the 'gbin.sh' file through the RPi2 terminal is:

```
sh gbin.sh {1} {2} {3} {4}
```

The four parameters are defined in Table 5.IV.

Table 5.IV: Parameter definitions for 'gbin.sh'.

Parameter	**Description**
{1}	transmitter antenna start number
{2}	transmitter antenna stop number
{3}	receiver antenna start number
{4}	receiver antenna stop number

An example of this command when using transmitter antennas 1-10 and antennas 11-20 as receiving,

```
sh gbin.sh 01 10 11 20
```

miniVNA PRO Software Parameters

The MVP software is executed within the ’gbin.sh’ shell script (refer to Appendix B.1) and the parameters can be changed by changing the following command within that script:

```
java Dconfigfile=gbin.xml -Dfstart={Start} -Dfstop={Stop} -Dfsteps={Steps}
-Dcalfile=gbin.cal -Dscanmode=TRAN -Dexports=csv -jar vnaJ-hl.3.1.3.jar
```

Where the following parameters are defined in Table 5.V.

Table 5.V: Parameter definitions for miniVNA PRO software command.

Parameter	**Description**
{Start}	Frequency range start (Hz)
{Stop}	Frequency range stop (Hz)
{Steps}	Number of Frequency steps

The command is set within the shell script by default as:

```
java Dconfigfile=gbin.xml -Dfstart=70000000 -Dfstop=100000000 -Dfsteps= 100
-Dcalfile=gbin.cal -Dscanmode=TRAN -Dexports=csv -jar vnaJ-hl.3.1.3.jar
```

Where the frequency range is 70-100MHz with 100 steps. The user can refer to the vnaJ Headless Software Manual [10] for additional information.

Chapter 6

Future Work

At the moment, the SPDAQ system is at an early stage of development. Our team has developed an Alpha prototype of the SPDAQ system for hardware and software testing in order to establish a proof of concept for this project. Although our team was successful in integrating the many hardware and software components for the system, there are still many things that can be improved on to make the system accessible to the general public. Initial designs for the SPDAQ system was to implement a battery operated device however due to project time constraints and project delays, this feature has yet to be implemented but should considered for future iterations. This chapter will explain the possible work that can be done to advance the current alpha prototype of the SPDAQ system and its individual components.

6.1 Software

As of now, the current software is at its very basic form where a shell script executes the SPDAQ software on the RPi2 with very little interface for the user to interact with. The user can edit certain files on the RPi2 in order to modify the settings which requires root access to the RPi2. This current method requires a good knowledge of the LINUX OS which is not commonly known by the average user. By implementing a more advanced GUI, the user can have more control over the SPDAQ system with an easier method to setup and configure any of the settings of the SPDAQ software. The GUI can also offer an easier method for the user to connect the RPi2 to the Internet for cloud services with a use of a Wifi adapter. To improve the software runtime, the use of another VNA that is open source should be considered in newer iterations of the SPDAQ system.

6.2 RF Multiplexer Module

At this stage, the RF Multiplexer component is currently being built and has yet to be tested. Through our SPDAQ prototype testing, we used an old RF Switch module provided by the EIL for the Alpha build. The RF Mux module designed by our team offers the same logistics as the RF Switch module provided by the EIL and therefore the upgrade to the newly designed RF Mux model, once manufactured, should be a simple transition. The work to be done once our RF Mux PCBs arrive will be to solder the RF switch integrated circuits (ICs) and to test with the rest of the SPDAQ Alpha prototype.

In terms of the DC switch, an addition that will simplify this automated process between the Raspberry Pi by and the DC switch, even in the case of software failure, would be by using a Serial Peripheral Interface (SPI) via a GPIO for the handshake process. This extended SPI communication will create more ports for the Arduino to use as well as provide a means for the software to not only talk to the Arduino, but also receive interrupt flags from the Arduino which can help in auto troubleshooting should anything go wrong during the process of data acquisition.

6.3 Antennna

The H-field antennas have been designed and tested. For the future, the E-Field antenna design will need to be modified in order to reduce cross-polarization so it can meet the SPDAQ system standards for a grain storage unit. Once modified, further tests need to be conducted with the antenna integrated with the SPDAQ system.

Chapter 7

Conclusions

The purpose of this project was to design a portable and affordable system for detecting moisture inside a grain bin using microwave imaging techniques. There were several different components comprising this system. Two types of antennas were studied; H-field and E-field antennas. A VNA was required for sending and receiving signals to and from the antennas and a multiplexer was required in order to connect the VNA to the array of antennas and perform the necessary switching. Also, a microprocessor and software was needed to provide control to the multiplexer and perform data acquisition and management.

It was found that the E-field antennas designed were not suitable for real world use for this application however the H-field antennas performed well. Due to time constraints and issues with our original supplier for our PCBs we were unable to complete the multiplexer in time for this report, however we hope to have something in time for our presentation. For testing our system we used an existing switch provided by EIL. The miniVNA PRO was a very affordable option but we were unable to get direct access to data obtained through it which resulted in our system being very slow in running through its data acquisition procedure. If direct access to this data were possible or a different VNA was used which allowed this direct access, our system would perform much quicker.

With a bit more work to complete with the multiplexer and resolving the issue with the limitation of the MVP's manufacturer software, we feel that we can succeed at creating an affordable and portable system for detecting moisture inside a grain bin.

References

[1] O.-A. R. Mohassel, "Doctoral committee: Professor chen-to tai, chairman," Ph.D. dissertation, The University of Michigan, 1982.

[2] S. Best and J. Morrow, "Limitations of inductive circuit model representations of meander line antennas," in *Antennas and Propagation Society International Symposium, 2003. IEEE*, vol. 1, June 2003, pp. 852–855 vol.1.

[3] K. Deng and M. Ma, "The study and implementation of meander-line antenna for an integrated transceiver design," 2010.

[4] P. Frost. (2015) What, if anything, makes shielded loop antennas so great at rejecting local noise. [Online]. Available: http://electronics.stackexchange.com/questions/70262/what-if-anything-makes-shielded-loop-antennas-so-great-at-rejecting-local-nois

[5] R. J. Spiegel, C. A. Booth, and E. L. Bronaugh, "A radiation measuring system with potential automotive under-hood application," *Electromagnetic Compatibility, IEEE Transactions on*, no. 2, pp. 61–69, 1983.

[6] R. Hartley. (2015) Rf / microwave pc board design and layout. [Online]. Available: http://www.qsl.net/va3iul/

[7] mRS mini Radio Solutions. (2015) minivna pro. [Online]. Available: http://miniradiosolutions.com/minivna-pro

[8] R. P. Foundation. (2015) Raspberry pi 2 model b. [Online]. Available: http://www.raspberrypi.org/products/raspberry-pi-2-model-b/

[9] D. Krause, *vna/J 3.1.4 User guide*, 2015. [Online]. Available: http://download.dl2sba.com/vnaj/manuals/UserGuide.pdf

[10] ——, *vna/J 3.x User guide for headless application*, 2015. [Online]. Available: http://download.dl2sba.com/vnaj/manuals/UserGuide.headless.pdf

[11] A. Fabrizi, "Dropbox uploader," 2014. [Online]. Available: https://github.com/andreafabrizi/Dropbox-Uploader

[12] Pi.gadgetoid.com. (2014) Raspberry pi pinout - rev 2 board. [Online]. Available: http://pi.gadgetoid.com/pinout

Appendix A

Budget

Table A.I: Project Budget

SYSTEM MODULE	COMPONENT	Supplier	Part No.	Price/Unit	Quantity	Sponsor	Estimated Cost	Actual Order Cost	Order Status
Antenna Array	Antenna PCBs					EIL	$300.00	$0.00	Process of ordering.
	Metallic rods								
Vector Network Analyzer (VNA)	MiniVNA Pro				1	EIL	$600.00	$0.00	Provided by EIL.
RF Multiplexer	MUX/DEMUX	Digikey	296-2057-5-ND	$0.43	6	EIL	$2.56	$0.00	Provided by EIL.
	SMA board edge	Digikey	J502-ND	$4.12	38	EIL	$156.42	$0.00	Provided by EIL.
	SMA board edge	Digikey	501-1381-ND	$6.06	5	EIL	$30.30	$0.00	Provided by EIL.
	SMA-SMA cable	Digikey	744-1374-ND	$9.40	6	EIL	$56.42	$0.00	Provided by EIL.
	cap 10nF 0805	Digikey	587-1113-1-ND	$0.34	50	EIL	$16.79	$0.00	Provided by EIL.
	cap 100nF 0805	Digikey	587-1133-6-ND	$0.16	100	EIL	$16.06	$0.00	Provided by EIL.
	SPDT	Digikey	HMC194MS8	$3.26	24	EIL	$78.24	$0.00	Provided by EIL.
	SP3T	Digikey	HMC245QS16	$4.13	2	EIL	$8.26	$0.00	Provided by EIL.
	SP8T	Digikey	HMC253QS24	$10.28	6	EIL	$61.68	$0.00	Provided by EIL.
	Arduino	Newark	45W6205	$40.21	1	EIL	$40.21	$0.00	Provided by EIL.
	RF Multiplexer PCBs	SeeedStudio		$10/board	5	EIL	$80.00	$0.00	Process of ordering.
				$6/board	5				
Controller	Raspberry Pi B+	Newark	68X0156	$43.60	1	ECE	$43.60	$43.60	Order placed and received.
	8GB microSD card								
	Raspberry Pi 2	Newark	38Y6467	$39.99	1	ECE	$39.99	$39.99	Order placed and received.
MISC.	Electrical components (wiring, resistors, capacitors, etc.)					ECE	$100.00		
	Machine Time	U of M			8 hrs.		$0.00		
							ECE	EIL	Project Total
						Subtotal	$83.59	$1446.94	$1530.53
						13% taxes	$10.87	$188.10	$198.97
						Shipping	$8	$160.11	$168.11
						Total	$102.46	$1795.15	$1897.61

Appendix B

S-Parameter Data Acquisition System Software

B.1 gbin.sh

Code B.1: S-Parameter Data Acquisition Shell Script Software

```bash
#!/bin/bash
if [ ! -f vnaJ-hl.3.1.3.jar ];
then
    echo ERROR! Missing vnaJ file...
    exit
fi

if [ -z $(lsusb | grep -e "Future Technology Devices") ];
then
    echo ERROR! MiniVNA Pro not connected...
fi

if [ $# -lt 4 ];
then
    echo ERROR! Missing parameters...
    exit
fi

if [ -z $(lsusb | grep -e "Arduino") ];
then
     echo ERROR! Arduino not connected...
```

```
else
    echo Tx: $1 - $2
    echo Rx: $3 - $4
    stty -F /dev/ttyACM0 cs8 9600 ignbrk -brkint -imaxbel -opost -onlcr -isig -icanon -iexten -echo -echoe -echok -echoctl -echoke noflsh -ixon -crtscts -hupcl

    for i in $(seq $1 $2)
    do
        if [ "$i" -lt 10 ];
        then
            echo sending 0$i to arduino...
            echo -n "0$i" > /dev/ttyACM0
        else
            echo sending $i to arduino...
            echo -n "$i" > /dev/ttyACM0
        fi

        echo changing transmitter to $i

        for j in $(seq $3 $4)
        do
            echo -n "$j" > /dev/ttyACM0
                echo changing reciever to $j

            echo Running vnaJ-hl.3.1.3.jar...
            nohup java -Dconfigfile=gbin.xml -Dfstart=70000000 -Dfstop=100000000 -Dfsteps=100 -Dcalfile=gbin.cal -Dscanmode=TRAN -Dexports=csv -jar vnaJ-hl.3.1.3.jar > log.txt
            path="vnaJ.3.1/export"

                #renaming exported file for post-processing
                [ "$i" -lt 10 ] && tx="0$i"|| tx="$i"
            rcvr=$(expr $j - 24)
            [ "$rcvr" -lt 10 ] && rx="0$rcvr"|| rx="$rcvr"
            mv ${HOME}/$path/gbin.cal.csv /${HOME}/$path/gbin_"$tx$rx".csv
        done
    done
fi

```

```
#running post-processing process
mono put2str.exe

#delete all exported miniVNA files after post-processing is done
rm -R ${HOME}/$path/*

#upload to linked dropbox
./dropbox_uploader.sh /root/grainbin/output output
```

B.2 put2str.cs

Code B.2: Post-Data Processing Program

```
using System.Linq;
using System.IO;
using System.Collections;
using System.Collections.Generic;

using System;
using System.Text;

class put2string{

  static string[,] sp = new string[256, 3];

  public static void Main(string[] args)
  {
      string path = @"/root/vnaJ.3.1/export";


      if(Directory.Exists(path))
          ProcessDirectory(path);
      else
          Console.WriteLine("{0} is not a valid directory.", path);

      List<string> linesToWrite = new List<string>();
      for(int rowIndex = 0; rowIndex < 256; rowIndex++)
      {
          StringBuilder line = new StringBuilder();
```

```
        for(int colIndex = 0; colIndex < 3; colIndex++)
            line.Append(sp[rowIndex, colIndex]).Append("\t");
        linesToWrite.Add(line.ToString());
    }

    //export file to sp.dat
    System.IO.File.WriteAllLines(@"/root/grainbin/output/sp.dat",
       linesToWrite.ToArray());
}

  // Process all files in the directory passed in
  public static void ProcessDirectory(string targetDirectory)
  {
      // Process the list of files found in the directory.
      string [] fileEntries = Directory.GetFiles(targetDirectory,
         "*.csv");
      if(fileEntries.Length == 0)
          Console.WriteLine("ERROR! No files in directory to
             process");
      else{
              int count = 0;
              foreach(string fileName in fileEntries)
              {
                string dataID =
                   Path.GetFileNameWithoutExtension(fileName);
                string tx = dataID.Substring(dataID.Length-4,2);
                string rx = dataID.Substring(dataID.Length-2,2);
                sp[count, 0] = tx;
                sp[count, 1] = rx;
                // Console.WriteLine("TX: {0}\tRX: {1}",
                   sp[count, 0], sp[count, 1]);
                ProcessFile(fileName, count);
                count++;
              }
      }
  }

  // Insert logic for processing found files here.
  public static void ProcessFile(string file, int count)
  {
      string[] lines = System.IO.File.ReadAllLines(file);
      string data = "";
```

```
        foreach(string line in lines.Skip(1)){

          string[] val = line.Split(',');

          double magdb = Convert.ToDouble(val[1]);
          double ph = Convert.ToDouble(val[2]);
          double mag = Math.Pow(10, magdb/20);
          double a = mag*Math.Cos(Math.PI*ph/180);
          double b = mag*Math.Sin(Math.PI*ph/180);

          data = string.Concat(data, string.Concat(a.ToString("N7")
             + "\t", b.ToString("N7") + "\t"));

          sp[count, 2] = data;
        }

        // Console.WriteLine("Processed file '{0}'.", file);
    }
  }
```

B.3 button.py

Code B.3: Button and LED function on Raspberry Pi 2

```
import RPi.GPIO as GPIO
from time import sleep
from sys import exit
import os

# to use Raspberry Pi board pin numbers
GPIO.setmode(GPIO.BCM)

# set up the GPIO channels - one input and one output
GPIO.setup(17, GPIO.IN) #push button
GPIO.setup(23, GPIO.OUT) #led

# input from pin 11
#input_value = GPIO.input(17)

try:
  while True:
    # output to pin 12
    if(GPIO.input(17) == True):
      #print("ON!")
      GPIO.output(23, True)
      sleep(0.5)
      GPIO.output(23, False)
      sleep(0.5)
      os.system("sh gbintest.sh 18 18 45 50")
     #else:
      #print("OFF!")

finally: GPIO.cleanup()
```

B.4 Dropbox Setup on the Raspberry Pi 2

The instructions below shows how a user can setup Dropbox on the Raspberry Pi 2 and how it can be linked to their Dropbox account. Note that an Internet connection is required for this installation. For more information on the Dropbox Uploader shell script, please refer to Andrea Fabriz's Github [11].

B.4.1 Setup Instructions

1. The Dropbox shell script can be downloaded using the following command:

   ```
   $ wget https://raw.github.com/andreafabrizi/Dropbox-Uploader/master/dropbox_uploader.sh$
   ```

2. Permissions on the shell script will need to be changed to make it executable. This can be done by the following command:

   ```
   $ chmod +x dropbox_uploader.sh
   ```

3. Now Dropbox can be configured for the first time by running

   ```
   $ ./dropbox_uploader.sh
   ```

4. Follow the instructions on the screen to create a new Dropbox app on your account from another web browser. Copy the app key and app secret given by Dropbox after filling out the create a new app form to the terminal window that is running the Dropbox shell script.
5. If the given information is correct, you will receive a oAUTH URL to enter into your web browser to verify app access to your Dropbox.
6. Dropbox on the Raspberry Pi 2 is now linked to your account. See below for Dropbox commands that can run on the Raspberry Pi 2.

B.4.2 'dropbox-uploader.sh' Commands

$< file/folder >$ is a required parameter
$[file/folder]$ is an option parameter

```
./dropbox-uploader.sh upload <LOCAL_FILE/DIR ...> <REMOTE_FILE/DIR>

./dropbox-uploader.sh download <REMOTE_FILE/DIR> [LOCAL_FILE/DIR]

./dropbox-uploader.sh delete <REMOTE_FILE/DIR>

./dropbox-uploader.sh move <REMOTE_FILE/DIR> [REMOTE_FILE/DIR]

./dropbox-uploader.sh copy <REMOTE_FILE/DIR> [REMOTE_FILE/DIR]

./dropbox-uploader.sh mkdir <REMOTE_DIR>

./dropbox-uploader.sh list <REMOTE_DIR>

./dropbox-uploader.sh share <REMOTE_DIR>

./dropbox-uploader.sh info

./dropbox-uploader.sh unlink
```

Appendix C

Raspberry Pi 2 Pinout

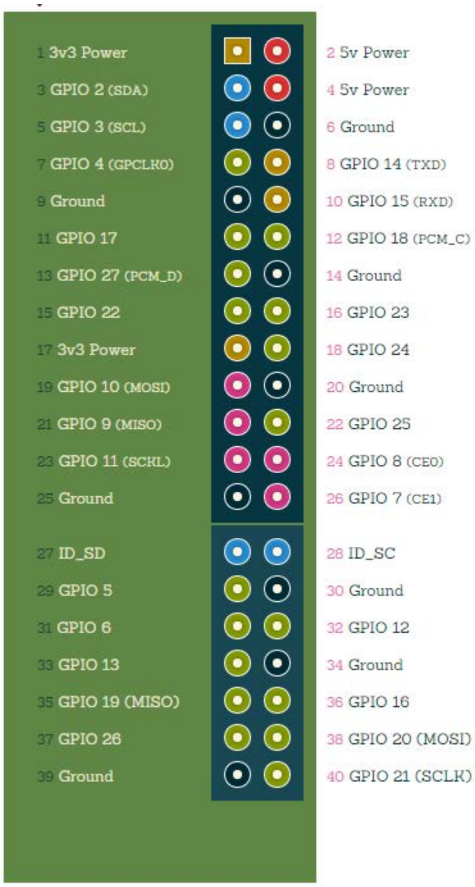

Fig. C.1: Raspberry Pi 2 Pinout [12].

Appendix D

DC Switch Lookup Tables

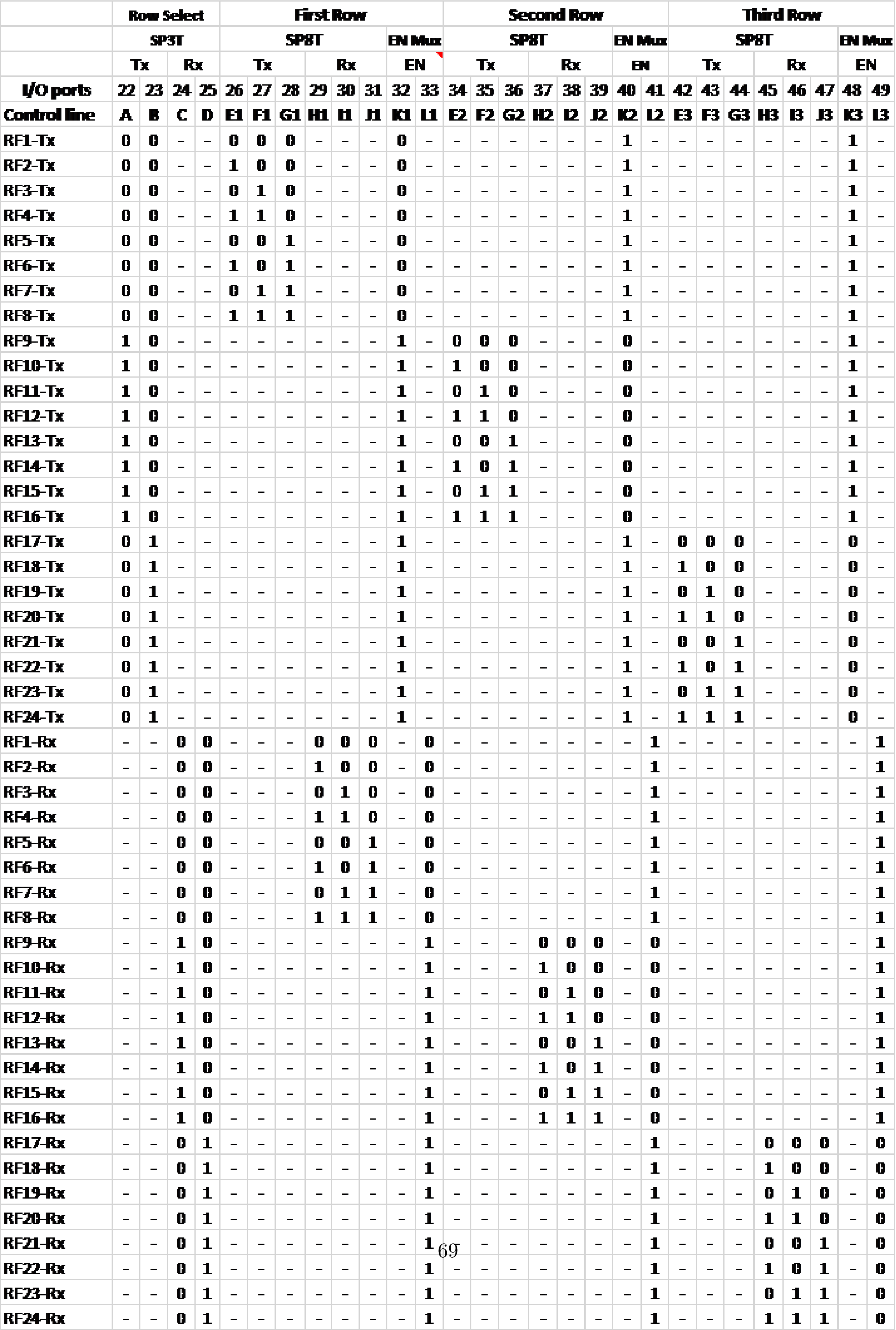

	Row Select				First Row								Second Row								Third Row							
	SP3T				SP8T						EN Mux		SP8T						EN Mux		SP8T						EN Mux	
	Tx		Rx		Tx			Rx			EN		Tx			Rx			EN		Tx			Rx			EN	
I/O ports	22	23	24	25	26	27	28	29	30	31	32	33	34	35	36	37	38	39	40	41	42	43	44	45	46	47	48	49
Control line	A	B	C	D	E1	F1	G1	H1	I1	J1	K1	L1	E2	F2	G2	H2	I2	J2	K2	L2	E3	F3	G3	H3	I3	J3	K3	L3
RF1-Tx	0	0	-	-	0	0	0	-	-	-	0	-	-	-	-	-	-	-	1	-	-	-	-	-	-	-	1	-
RF2-Tx	0	0	-	-	1	0	0	-	-	-	0	-	-	-	-	-	-	-	1	-	-	-	-	-	-	-	1	-
RF3-Tx	0	0	-	-	0	1	0	-	-	-	0	-	-	-	-	-	-	-	1	-	-	-	-	-	-	-	1	-
RF4-Tx	0	0	-	-	1	1	0	-	-	-	0	-	-	-	-	-	-	-	1	-	-	-	-	-	-	-	1	-
RF5-Tx	0	0	-	-	0	0	1	-	-	-	0	-	-	-	-	-	-	-	1	-	-	-	-	-	-	-	1	-
RF6-Tx	0	0	-	-	1	0	1	-	-	-	0	-	-	-	-	-	-	-	1	-	-	-	-	-	-	-	1	-
RF7-Tx	0	0	-	-	0	1	1	-	-	-	0	-	-	-	-	-	-	-	1	-	-	-	-	-	-	-	1	-
RF8-Tx	0	0	-	-	1	1	1	-	-	-	0	-	-	-	-	-	-	-	1	-	-	-	-	-	-	-	1	-
RF9-Tx	1	0	-	-	-	-	-	-	-	-	1	-	0	0	0	-	-	-	0	-	-	-	-	-	-	-	1	-
RF10-Tx	1	0	-	-	-	-	-	-	-	-	1	-	1	0	0	-	-	-	0	-	-	-	-	-	-	-	1	-
RF11-Tx	1	0	-	-	-	-	-	-	-	-	1	-	0	1	0	-	-	-	0	-	-	-	-	-	-	-	1	-
RF12-Tx	1	0	-	-	-	-	-	-	-	-	1	-	1	1	0	-	-	-	0	-	-	-	-	-	-	-	1	-
RF13-Tx	1	0	-	-	-	-	-	-	-	-	1	-	0	0	1	-	-	-	0	-	-	-	-	-	-	-	1	-
RF14-Tx	1	0	-	-	-	-	-	-	-	-	1	-	1	0	1	-	-	-	0	-	-	-	-	-	-	-	1	-
RF15-Tx	1	0	-	-	-	-	-	-	-	-	1	-	0	1	1	-	-	-	0	-	-	-	-	-	-	-	1	-
RF16-Tx	1	0	-	-	-	-	-	-	-	-	1	-	1	1	1	-	-	-	0	-	-	-	-	-	-	-	1	-
RF17-Tx	0	1	-	-	-	-	-	-	-	-	1	-	-	-	-	-	-	-	1	-	0	0	0	-	-	-	0	-
RF18-Tx	0	1	-	-	-	-	-	-	-	-	1	-	-	-	-	-	-	-	1	-	1	0	0	-	-	-	0	-
RF19-Tx	0	1	-	-	-	-	-	-	-	-	1	-	-	-	-	-	-	-	1	-	0	1	0	-	-	-	0	-
RF20-Tx	0	1	-	-	-	-	-	-	-	-	1	-	-	-	-	-	-	-	1	-	1	1	0	-	-	-	0	-
RF21-Tx	0	1	-	-	-	-	-	-	-	-	1	-	-	-	-	-	-	-	1	-	0	0	1	-	-	-	0	-
RF22-Tx	0	1	-	-	-	-	-	-	-	-	1	-	-	-	-	-	-	-	1	-	1	0	1	-	-	-	0	-
RF23-Tx	0	1	-	-	-	-	-	-	-	-	1	-	-	-	-	-	-	-	1	-	0	1	1	-	-	-	0	-
RF24-Tx	0	1	-	-	-	-	-	-	-	-	1	-	-	-	-	-	-	-	1	-	1	1	1	-	-	-	0	-
RF1-Rx	-	-	0	0	-	-	-	0	0	0	-	0	-	-	-	-	-	-	-	1	-	-	-	-	-	-	-	1
RF2-Rx	-	-	0	0	-	-	-	1	0	0	-	0	-	-	-	-	-	-	-	1	-	-	-	-	-	-	-	1
RF3-Rx	-	-	0	0	-	-	-	0	1	0	-	0	-	-	-	-	-	-	-	1	-	-	-	-	-	-	-	1
RF4-Rx	-	-	0	0	-	-	-	1	1	0	-	0	-	-	-	-	-	-	-	1	-	-	-	-	-	-	-	1
RF5-Rx	-	-	0	0	-	-	-	0	0	1	-	0	-	-	-	-	-	-	-	1	-	-	-	-	-	-	-	1
RF6-Rx	-	-	0	0	-	-	-	1	0	1	-	0	-	-	-	-	-	-	-	1	-	-	-	-	-	-	-	1
RF7-Rx	-	-	0	0	-	-	-	0	1	1	-	0	-	-	-	-	-	-	-	1	-	-	-	-	-	-	-	1
RF8-Rx	-	-	0	0	-	-	-	1	1	1	-	0	-	-	-	-	-	-	-	1	-	-	-	-	-	-	-	1
RF9-Rx	-	-	1	0	-	-	-	-	-	-	-	1	-	-	-	0	0	0	-	0	-	-	-	-	-	-	-	1
RF10-Rx	-	-	1	0	-	-	-	-	-	-	-	1	-	-	-	1	0	0	-	0	-	-	-	-	-	-	-	1
RF11-Rx	-	-	1	0	-	-	-	-	-	-	-	1	-	-	-	0	1	0	-	0	-	-	-	-	-	-	-	1
RF12-Rx	-	-	1	0	-	-	-	-	-	-	-	1	-	-	-	1	1	0	-	0	-	-	-	-	-	-	-	1
RF13-Rx	-	-	1	0	-	-	-	-	-	-	-	1	-	-	-	0	0	1	-	0	-	-	-	-	-	-	-	1
RF14-Rx	-	-	1	0	-	-	-	-	-	-	-	1	-	-	-	1	0	1	-	0	-	-	-	-	-	-	-	1
RF15-Rx	-	-	1	0	-	-	-	-	-	-	-	1	-	-	-	0	1	1	-	0	-	-	-	-	-	-	-	1
RF16-Rx	-	-	1	0	-	-	-	-	-	-	-	1	-	-	-	1	1	1	-	0	-	-	-	-	-	-	-	1
RF17-Rx	-	-	0	1	-	-	-	-	-	-	-	1	-	-	-	-	-	-	-	1	-	-	-	0	0	0	-	0
RF18-Rx	-	-	0	1	-	-	-	-	-	-	-	1	-	-	-	-	-	-	-	1	-	-	-	1	0	0	-	0
RF19-Rx	-	-	0	1	-	-	-	-	-	-	-	1	-	-	-	-	-	-	-	1	-	-	-	0	1	0	-	0
RF20-Rx	-	-	0	1	-	-	-	-	-	-	-	1	-	-	-	-	-	-	-	1	-	-	-	1	1	0	-	0
RF21-Rx	-	-	0	1	-	-	-	-	-	-	-	1	-	-	-	-	-	-	-	1	-	-	-	0	0	1	-	0
RF22-Rx	-	-	0	1	-	-	-	-	-	-	-	1	-	-	-	-	-	-	-	1	-	-	-	1	0	1	-	0
RF23-Rx	-	-	0	1	-	-	-	-	-	-	-	1	-	-	-	-	-	-	-	1	-	-	-	0	1	1	-	0
RF24-Rx	-	-	0	1	-	-	-	-	-	-	-	1	-	-	-	-	-	-	-	1	-	-	-	1	1	1	-	0

Fig. D.1

Appendix E

Curriculum Vitae

Dimitri Anistratov

PLACE OF BIRTH:	Winnipeg, Manitoba
YEAR OF BIRTH:	1991
SECONDARY EDUCATION:	University of Manitoba(2009 -2015)

Robert Brandt

PLACE OF BIRTH:	Winnipeg, Manitoba
YEAR OF BIRTH:	1979
SECONDARY EDUCATION:	University of Manitoba(2010 -2015)
HONOUR AND AWARDS:	Dean's Honor Roll 2010

Shucheng Gu

PLACE OF BIRTH: Nanjing China
YEAR OF BIRTH: 1990
SECONDARY EDUCATION: University of Manitoba(2010 -2015)
HONOUR AND AWARDS: Dean's Honor Roll 2010

Kathy Nguyen

PLACE OF BIRTH: Winnipeg, Manitoba
YEAR OF BIRTH: 1989
SECONDARY EDUCATION: University of Manitoba(2010 -2015)

Edinam Tettevi

PLACE OF BIRTH:	Accra, Ghana
YEAR OF BIRTH:	1989
SECONDARY EDUCATION:	University of Manitoba(2010 -2016)
HONOUR AND AWARDS:	MTS Mobility Scholarships 2011 International Undergraduate Student Scholarship Dept. of Development & Advancement Services Scholarship University 1 Honor List Fall 2010 University 1 Honor List Winter 2011 Dean's Honor List Fall 2013